



Ferric Sulfasalazine Sulfa Drug Complex Supported on Cobalt Ferrite Cellulose; Evaluation of Its Activity in MCRs

Shahnaz Rostamizadeh¹ · Zahra Daneshfar¹ · Ali Khazaei¹

Received: 3 September 2019 / Accepted: 9 January 2020
© Springer Science+Business Media, LLC, part of Springer Nature 2020

Abstract

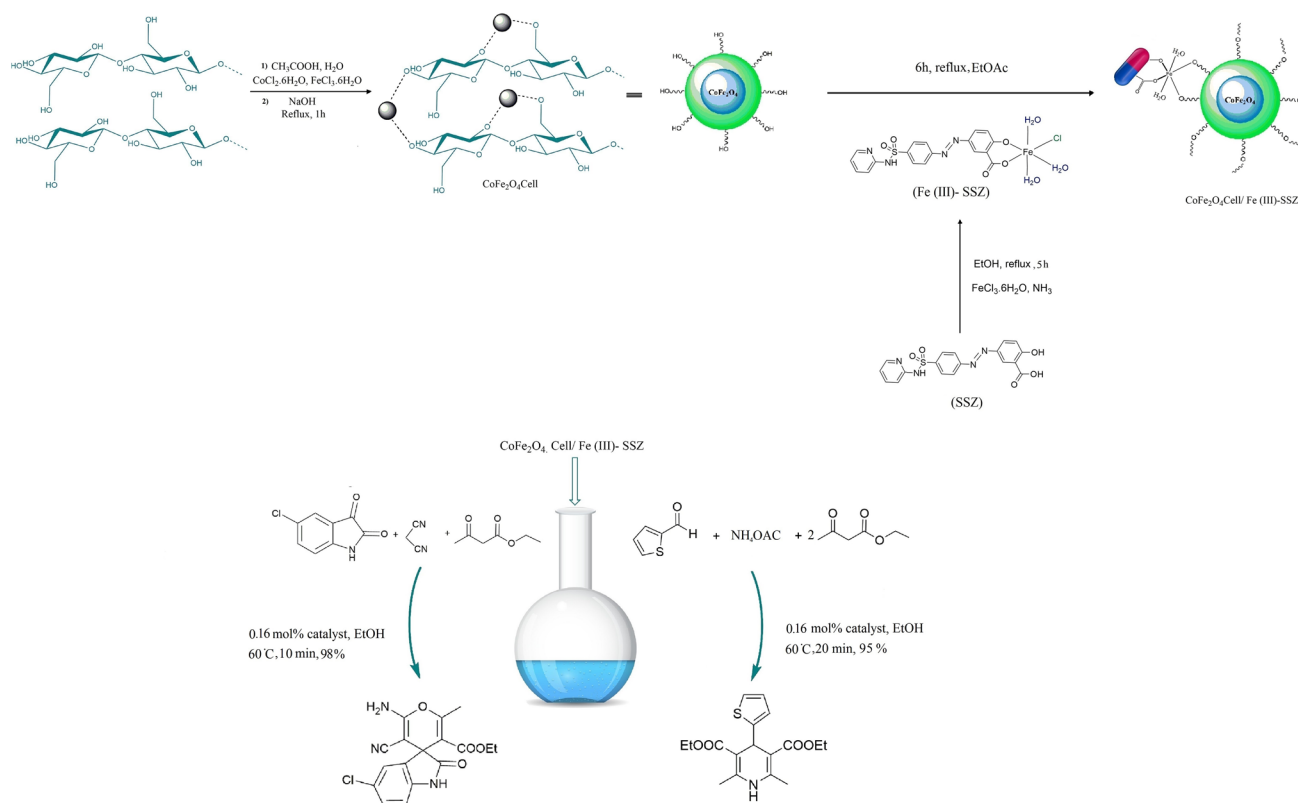
The green and nano catalyst was simply prepared through the reaction of ferric sulfasalazine with nanomaterial CoFe_2O_4 -cellulose as a magnetic biopolymer surface. This novel heterogeneous organometallic catalyst was characterized by X-ray diffraction, field emission scanning electron microscopy, FT-IR spectroscopy, thermal gravimetric analysis, and energy dispersive analysis of X-rays, and inductively coupled plasma-mass spectrometry. This green sulfasalazine drug complex supported on CoFe_2O_4 cellulose was applied as an efficient and recyclable catalyst for organic reactions such as synthesis of functionalized 4H- pyrans and 1,4-dihydropyridines derivatives. All of the reactions were carried out successfully under mild conditions in a short reaction time. The used catalyst was easily separated and reused for 6 runs without noticeable loss of its catalytic activity.

Electronic supplementary material The online version of this article (doi:<https://doi.org/10.1007/s10562-020-03101-6>) contains supplementary material, which is available to authorized users.

✉ Shahnaz Rostamizadeh
rostamizadeh@kntu.ac.ir

¹ Department of Chemistry, Faculty of Science, K. N. Toosi University of Technology, P.O. Box 15875-4416, Tehran, Iran

Graphic Abstract



Keywords Sulfasalazine · Organometallic complex · Green chemistry · Magnetic catalyst · Heterogenic catalyst · Cellulose

1 Introduction

Green chemistry as a critical and important major subject in science and environment has increased the application of recyclable heterogeneous acids which can be used instead of harsh and non-reusable liquid acid catalysts like: hydrochloric acid, sulfuric acid and etc. Therefore, these days application of novel solid acid catalysts has been increased [2]. Also it is notable that organometallic complexes have been recognized to perform as effective catalysts in organic reactions [8, 22] and also with important bioactive properties [29]. In recent reports, metal carboxylates have been extensively studied not only due to their interesting electro-conductive, optical and magnetic properties [10], but also because the carboxylic group can bind to metal ions in various modes, such as monodentate, bidentate, and bridging [28]. One important example of these ligands with ability to form the metal complexes is salicylic acid. From the coordination chemistry view point, salicylic acid is a useful ligand for chelating with metal ions. It can offer two hard and strong basic O-donor centers either from both of carboxyl and hydroxyl groups or only from the carboxyl group

as a bidentate chelator [25]. Copper (II) complex of salicylic acid catalyzed cross-coupling reactions [7]. There is currently much interest in iron (III) salicylate complex, for its applications in biomedicine and environmental monitoring [23, 24, 26]. One important derivative of salicylic acid is sulfasalazine drug. Sulfasalazine as an important sulfa drug under the trade name Azulfidine is used to treat rheumatoid arthritis, ulcerative colitis, and Crohn's diseases [18]. Also due to its ability to form stable complexes, a series of sulfasalazine complexes with different metals such as: Fe (III), Co (II), Ni (II), Cu (II), Zn (II) and Cd (II) were reported recently [34]. Based on the principle of green chemistry, heterogeneous catalysts have some advantageous over homogeneous catalysts. They can be recovered from the reaction mixture through filtration or centrifugation and reused after activation. Thus it makes the process economically possible [43, 44] Also heterogenization of organometallic compounds through attaching them to inorganic or organic supports is the most general method. Therefore a lot of approaches have been established to attach complexes to different solids such as covalent anchoring, electrostatic adsorption, ship-in-a bottle and supported liquid phase [36]. Magnetic

nanoparticles (MNPs) are probably the most generally considered compared to other supports like silica, alumina, activated carbon, metal oxides, zeolites and polymers. It is as an excellent and ideal support with significant industrial potential due to its extraordinary properties such as having large specific surface area, being readily dispersed in reaction solution, and easy functionalization with various groups [13]. Their super-paramagnetic character makes them effective and easily recovered from the reaction mixture via an external permanent magnet. Therefore, a wide range of the magnetically recyclable, nano catalysts with excellent catalytic activities have been developed [4, 6, 39–41, 43, 44]. Among the various MNPs as the core magnetic supports, cobalt ferrite is one of the most versatile magnetic materials. It has moderated saturation magnetization, high chemical stability and mechanical strength [27]. Also, cellulose is an important natural material in the world. This biodegradable polymer has an important role as a biocompatible and renewable resource containing hydroxyl groups [33]. The presence of a great number of hydroxyl groups makes it possible to attach to MNPs ions through chelation mechanism without using any linkers [38]. Hence, through the combination of the properties of cobalt ferrite with cellulose, the development of novel, highly active and reusable immobilized catalyst is improved [43, 44]. Based on the literature reports, magnetic cellulose has been linked to different metals such as copper (II) and titanium (I) via its hydroxyl groups [3, 30]. Also, ferric ion as a safe and eco-friendly cation is a good Lewis acid which is able to activate carbonyl groups for nucleophilic addition reactions. Thus, the main purpose of the present work is to prepare a new, bio-based magnetic, nano heterogeneous and organometallic catalyst which is “CoFe₂O₄@nano-cellulose/Fe (III)-SSZ”.

It is worth mentioning that multicomponent reactions (MCRs) containing domino processes have developed as potent tools to extent this important issue. Such transformations reduce the use of catalyst, solvent, time, and energy [17, 42]. One of these MCRs is to synthesis 1,4-dihydropyridine (DHP) derivatives contain a large family of medically important compounds with diverse pharmacological and therapeutic properties [12]. Although the synthesis of DHPs has been carried out by a variety of homogeneous and heterogeneous catalysts, some of these methods suffer from limited scope like low yields, long reaction time, expensive catalysts and difficult work-up procedures [9, 15, 20, 31, 32, 35]. Another multicomponent reaction is preparing 4H-pyrans derivatives. 4H-pyrans and their derivatives are considerable due to their pharmacological activities [14], for instance spasmolytic, diuretic, anticoagulant, anticancer, and anti-anaphylactic [1, 5, 37]. Many methods for the synthesis of 4H-pyrans have been reported in the literature. Although, these methods have their own advantages, but they still have significant limitations like harsh reaction conditions, long

reaction time and use of expensive, unavailable catalysts [11, 16, 19, 21]. Also for synthesis of 4H-pyrans derivatives usually basic homogeneous catalysts were applied. So applying an inexpensive, heterogeneous and acidic catalyst could be worthwhile. These findings led us to do an efficient and green process for synthesis of these ring systems. In this article efficient methodologies were described for the synthesis of 4H-pyran and DHP derivatives using “CoFe₂O₄@nano-cellulose/Fe (III) SSZ” as a green heterogeneous catalyst.

2 Experimental

2.1 Materials

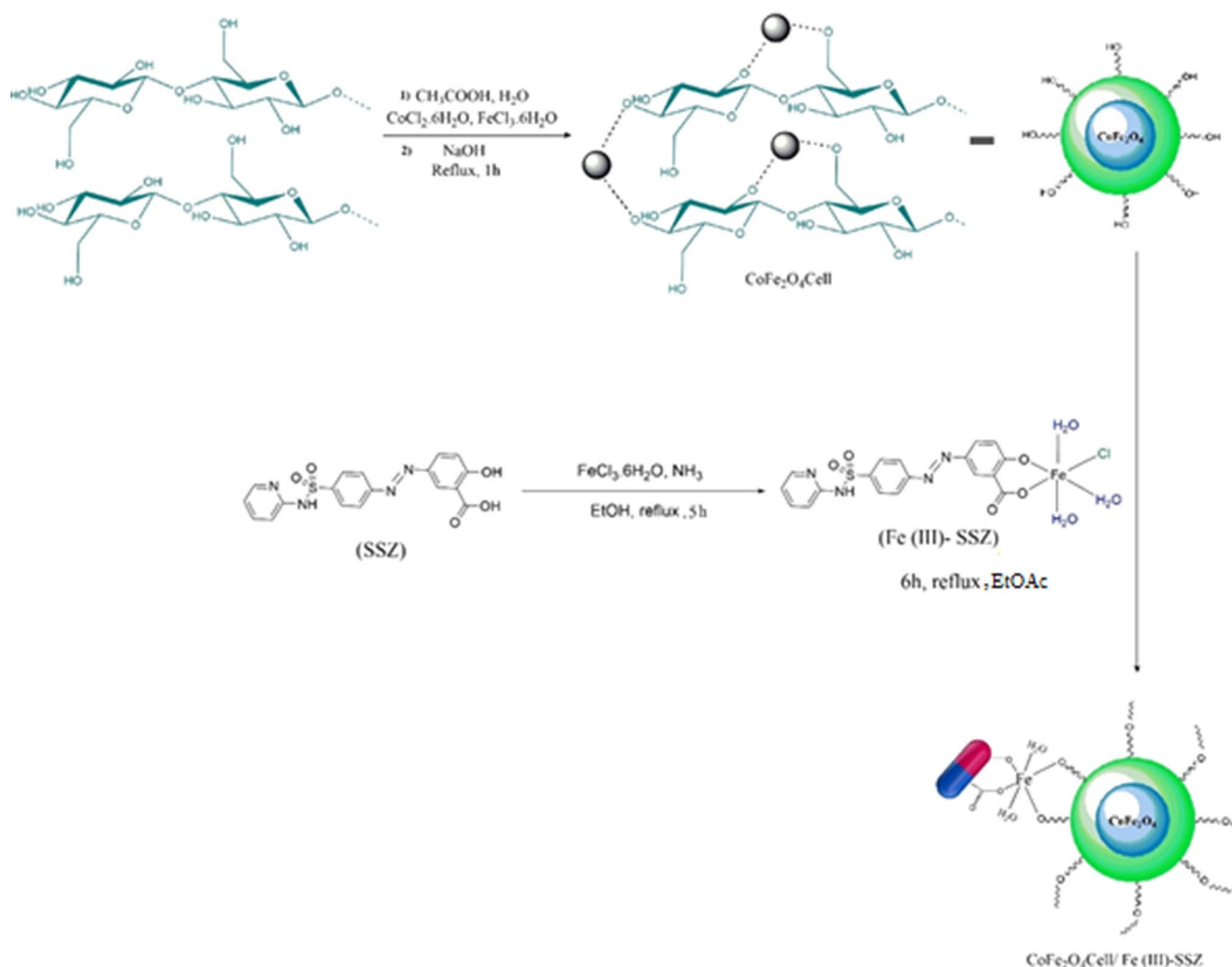
All materials were purchased from Sigma-Aldrich Company.

2.2 Preparation and Characterization of CoFe₂O₄-Cell-Fe (III)/SSZ

The magnetic CoFe₂O₄ cellulose/ferric (III) sulfasalazine nanoparticles were prepared in three steps as presented in Scheme 1. The first step was preparing magnetic CoFe₂O₄-cellulose nanoparticles by a one-pot synthesis method. Cellulose was dissolved in a 3% acetic acid solution, then an aqueous solution of FeCl₃ 6H₂O and CoCl₂ 6H₂O was added. The mixture was stirred vigorously for 2 h, and then a sodium hydroxide solution was added [43, 44]. The second step was to prepare ferric (III) sulfasalazine. It was carried out by reaction of ferric chloride to a hot mixture of ammonia and ethanol solution of sulfasalazine for the mono complexation [34]. Then, CoFe₂O₄Cell presented a support for the immobilization of ferric sulfasalazine by the reaction of hydroxyl groups of cellulose with ferric chloride complexed with sulfasalazine acid. Ferric sulfasalazine at reflux conditions in ethyl acetate was attached to CoFe₂O₄Cell nanoparticles. The content of ferric ion complexed to sulfasalazine supported on CoFe₂O₄-Cell was 0.16 mmol.g⁻¹ determined by ICP-MS. Also, the EDAX analysis of this catalyst showed elimination of the chloride ion. The preparation of CoFe₂O₄Cell/ Fe (III) SSZ was described in Scheme 1 (For more information see ESI).

2.3 General Procedure for the 4H- Pyrans Derivatives Synthesis

A suspension of malonitrile (1 mmol), ethyl acetoacetate (methyl acetoacetate, acetoacetate) (1 mmol), aldehyde (1 mmol) and the catalyst (0.01 g, 0.0016 mmol) in ethanol (10 ml) was stirred at 60 °C. After completion of the reaction which was monitored by TLC, the catalyst was separated by using an external magnet. The mixture was poured into



Scheme 1 The preparation of $\text{CoFe}_2\text{O}_4\text{Cell-Fe (III) SSZ}$

cold water and the precipitate was filtered. The solid was recrystallized with ethanol and dried in an oven at 60°C .

2.4 General Procedure for the 1, 4-DHP Derivatives Synthesis

In a 25 mL round-bottomed flask, aldehyde (1 mmol), ethyl acetoacetate (methyl acetoacetate, acetoacetate) (2 mmol), ammonium acetate (1 mmol), and the catalyst (0.01 g, 0.0016 mmol) in 10 ml ethanol were added. The reaction mixture was stirred at 60°C . After completion of the reaction which was traced by TLC, the catalyst was separated by using an external magnet. The pure product was obtained by crystallization of the crude material from ethanol.

2.5 Physical Measurements

Reactions were carried out under air condition. Melting points were measured on an Electro thermal 9200 apparatus.

Mass spectra were recorded on a Finnigan-MAT 8430 mass spectrometer operating at an ionization potential of 70 eV. IR Spectra were recorded on a Shimadzu IR-470 spectrometer. Proton nuclear magnetic resonance spectra (^1H NMR) were recorded on a Bruker DRX-300 Advance spectrometer 300.13 MHz; chemical shifts (δ scale) are reported in parts per million (ppm). ^1H NMR Spectra are reported in order: number of protons, multiplicity and approximate coupling constant (J value) in hertz (Hz); signals were characterized as s (singlet), d (doublet), t (triplet), m (multiplet), and br s (broad signal). The ^{13}C NMR spectra were recorded at 75.47 MHz and 100 MHz; chemical shifts (δ scale) are reported in parts per million (ppm). The elemental analyses were performed with an Elementar Analysensysteme GmbH Vario EL. Diffraction data were collected on a STOE STADI P with scintillation detector, secondary monochromator and Cu-K α 1 radiation ($\lambda = 1.5406 \text{ \AA}$). TG/DTA experiments were carried out by a BÄHR Thermo analysis with a temperature program from 10 to 800°C at a constant rate of

20 °C per min. Scanning electron microscopy was carried out by Philips XL-30 ESEM. Inductively coupled plasma-mass spectrometry was obtained using a Perkin–ElmerElan 600 quadrupole ICP-MS with a CetaxLSX-200 UV laser module.

3 Results and Discussion

The green and nano catalyst based on sulfasalazine drug was characterized by X-ray diffraction (XRD), field emission scanning electron microscopy (FE-SEM), FT-IR spectroscopy, thermal gravimetric analysis (TGA), energy dispersive analysis of X-rays (EDAX), and inductively coupled plasma-mass spectrometry (ICP-MS). In order to evaluate

the catalytic activity of $\text{CoFe}_2\text{O}_4\text{-Cell/Fe (III) SSZ}$, a one-pot synthesis of two different multi component reactions was chosen. First one was the reaction of malonitrile, aldehyde (or isatin) and ethyl acetoacetate (methyl acetoacetate or acetoacetone) to obtain 4H-pyrans. The second one was the reaction of ammonium acetate, aldehyde and ethyl acetoacetate (methyl acetoacetate or acetoacetone) to gain 1,4-dihydropyridines. Benzaldehyde was chosen as the model compound for the optimization of 4H-pyrans and 1,4-dihydropyridines synthesis.

3.1 XRD analysis

The XRD patterns of $\text{CoFe}_2\text{O}_4\text{@nano-cellulose/Fe (III) SSZ}$ and $\text{CoFe}_2\text{O}_4\text{Cell}$ were shown in Figs. 1 and 2. The XRD

Fig. 1 XRD pattern of $\text{CoFe}_2\text{O}_4\text{@ Cell/Fe (III)-SSZ}$

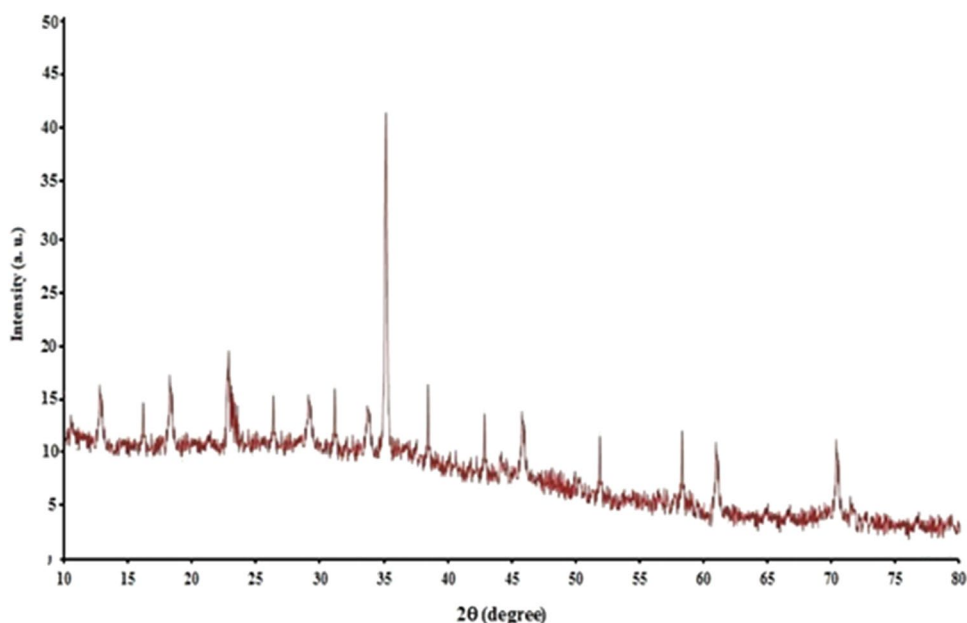
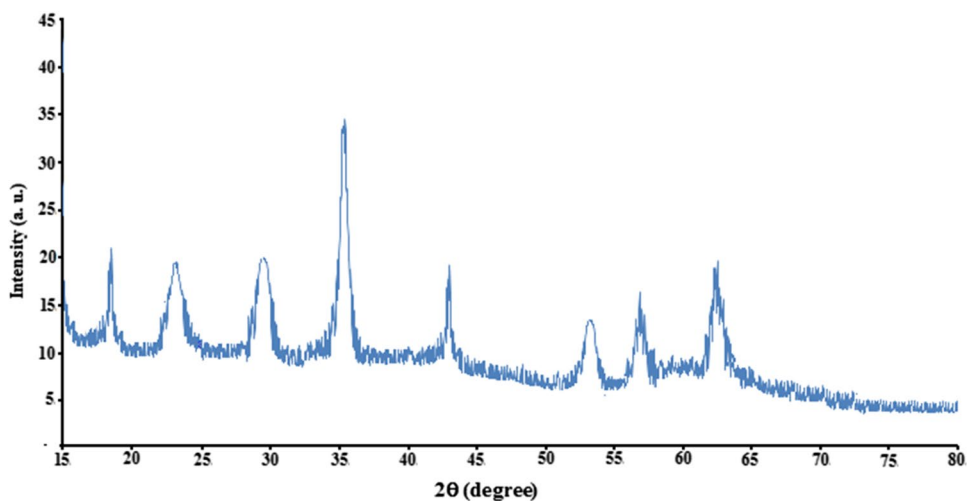


Fig. 2 XRD pattern of $\text{CoFe}_2\text{O}_4\text{@ Cell}$



pattern of CoFe_2O_4 @nano-cellulose/Fe (III)SSZ has shown diffraction peaks at $2\theta = 18.2^\circ$, 29.10° , 32.698° , 35.7935° , 43.42° , 57.51° and 61.78° with FWHM equal to 0.55, 0.56, 0.28, 0.42, 0.48, 0.23 and 0.53 respectively. They were quite matched with the cubic spinel structure of pure CoFe_2O_4 . Also these data were similar with the XRD of CoFe_2O_4 Cell. The diffraction peaks at $2\theta = 16.97^\circ$ and 26.25° with FWHM equal to 0.36 and 0.29 respectively, have shown the existence of cellulose. The observed signals at $2\theta = 23.81^\circ$ and 38.0607° with FWHM equal to 0.52 and 0.21 were related to Fe (III)-SSZ. Other signals in $2\theta = 13.68^\circ$, 34.25° and 45.71° , 53.94° and 70.16° with FWHM equal to 0.40, 0.57, 0.20, 0.22 and 0.51 exposed the existence of cellulose and connection of ferric ion to cellulosic shell (Table 1).

3.2 TEM and SEM Measurement

The morphology and size details of the nano catalyst were investigated by SEM measurement illustrated in Fig. 3. The SEM image of pure CoFe_2O_4 -Cell/Fe (III)-SSZ indicated that the diameter of its particles were around 45 nm. Both CoFe_2O_4 -Cell/Fe (III)-SSZ and CoFe_2O_4 Cell nanoparticles have a core-shell mode and spherical morphology. Also the TEM image shown in Fig. 3e and f indicate that magnetite composites served as supports for the catalyst. Furthermore it has appropriate spherical morphologies and regular core-shell structures.

3.3 EDAX and CHN Measurement

EDAX analysis of ferric sulfasalazine, CoFe_2O_4 Cell and CoFe_2O_4 Cell/ Fe (III)-SSZ were described in Table 2. The

presence of cobalt and ferric ions was obvious in CoFe_2O_4 @Cell (Table 2, entry 1). Based on EDAX, the presence of Cl and Fe in Fe (III) SSZ confirmed chelation of ferric ion to sulfasalazine (Table 2, entry 2). EDAX analysis of CoFe_2O_4 Cell/Fe (III)-SSZ demonstrated the presence of Co, Fe, N and S which means contribution of the sulfa drug organometal complex with the magnetic support (Table 2, entry 3). Notably, elimination of chloride in CoFe_2O_4 -Cell/Fe (III)-SSZ was confirmed (Table 2, entry 3) indicating the final structure of the catalyst. The EDAX analysis of CoFe_2O_4 Cell/Fe (III)-SSZ and CoFe_2O_4 Cell were demonstrated in Figs. 4 and 5. Also CHN analysis of cellulose, CoFe_2O_4 Cell, Fe (III)-SSZ and CoFe_2O_4 Cell/Fe (III)-SSZ were presented in Table 3. Based on the data, nitrogen in Fe (III)-SSZ and CoFe_2O_4 -Cell/Fe (III)-SSZ was obtainable (Table 3, entries 4 and 5). The percentages of C, H and N elements in cellulose, CoFe_2O_4 Cell and Fe (III)-SSZ were demonstrated in Fig. 5. Finally, a comparison of the elements for the reported substrates was obvious in Figs. 6 and 7.

3.4 FT-IR Analysis

The FTIR of cellulose (a), CoFe_2O_4 -Cell (b), SSZ (c), Fe (III)-SSZ (d) and CoFe_2O_4 -Cell/Fe (III)-SSZ (e) were shown in Fig. 8. The FT-IR spectrum of nano-cellulose (Fig. 8a) showed a broad band at 3338 cm^{-1} which was related to the stretching vibrations of hydroxyl groups. For CoFe_2O_4 -Cell (Fig. 8b) the absorption signals at 1058 and 1108 cm^{-1} displayed the stretching vibrations of the C–O bonds. In addition to the cellulose absorption bands, stretching vibrations of Fe–O and Co–O groups at 582 and 681 cm^{-1} were appeared. These signals indicated that the magnetic CoFe_2O_4 nano particles were coated by cellulose [43, 44]. The IR spectrum of sulfasalazine drug (Fig. 8c) showed a medium signal at 3438 cm^{-1} attributed to the phenolic OH and carboxylic OH groups. A strong peak in ferric sulfasalazine (M:L = 1:1), (Fig. 8d) at 1259 cm^{-1} was related to the shift of the $\nu(\text{C}=\text{O})$ of the phenolic group. The phenolic hydroxyl group was found deprotonated in the mono complexes, which was apparent from the absence of the $\sigma(\text{OH})$ in plane bending in 1394 cm^{-1} strongly [34]. The presence of water molecules in the complex was determined by the appearance of $\nu(\text{OH})$ as a broad peak in the range of $3500\text{--}3000\text{ cm}^{-1}$, and $\gamma(\text{OH})$ in the range of $965\text{--}914\text{ cm}^{-1}$. The other bending vibration of the water molecule $\sigma(\text{OH})$ was appeared around 1600 cm^{-1} , which always interferes with the skeleton vibration of the benzene ring (C=C vibration). The spectrum of Fe (III)-SSZ showed sharp peaks at 1616 and 1425 cm^{-1} assigned to asymmetric and symmetric stretching vibration of the carboxylate moiety, respectively. These two signals were either slightly shifted to lower frequencies indicating the participation of

Table 1 XRD analysis of CoFe_2O_4 @Cell/ Fe (III) SSZ

Entry	Position ($2\theta^\circ$)	FWHM ($2\theta^\circ$)
1	13.6815	0.4040
2	16.9791	0.3650
3	18.2	0.5512
4	23.8199	0.5210
5	26.2532	0.2914
6	29.1068	0.5600
7	32.698	0.2815
8	34.2572	0.5710
9	35.7935	0.4245
10	38.0607	0.2106
11	43.4246	0.4823
12	45.7114	0.2011
13	53.9425	0.2210
14	57.5101	0.2300
15	61.7800	0.5310
16	70.1670	0.5120

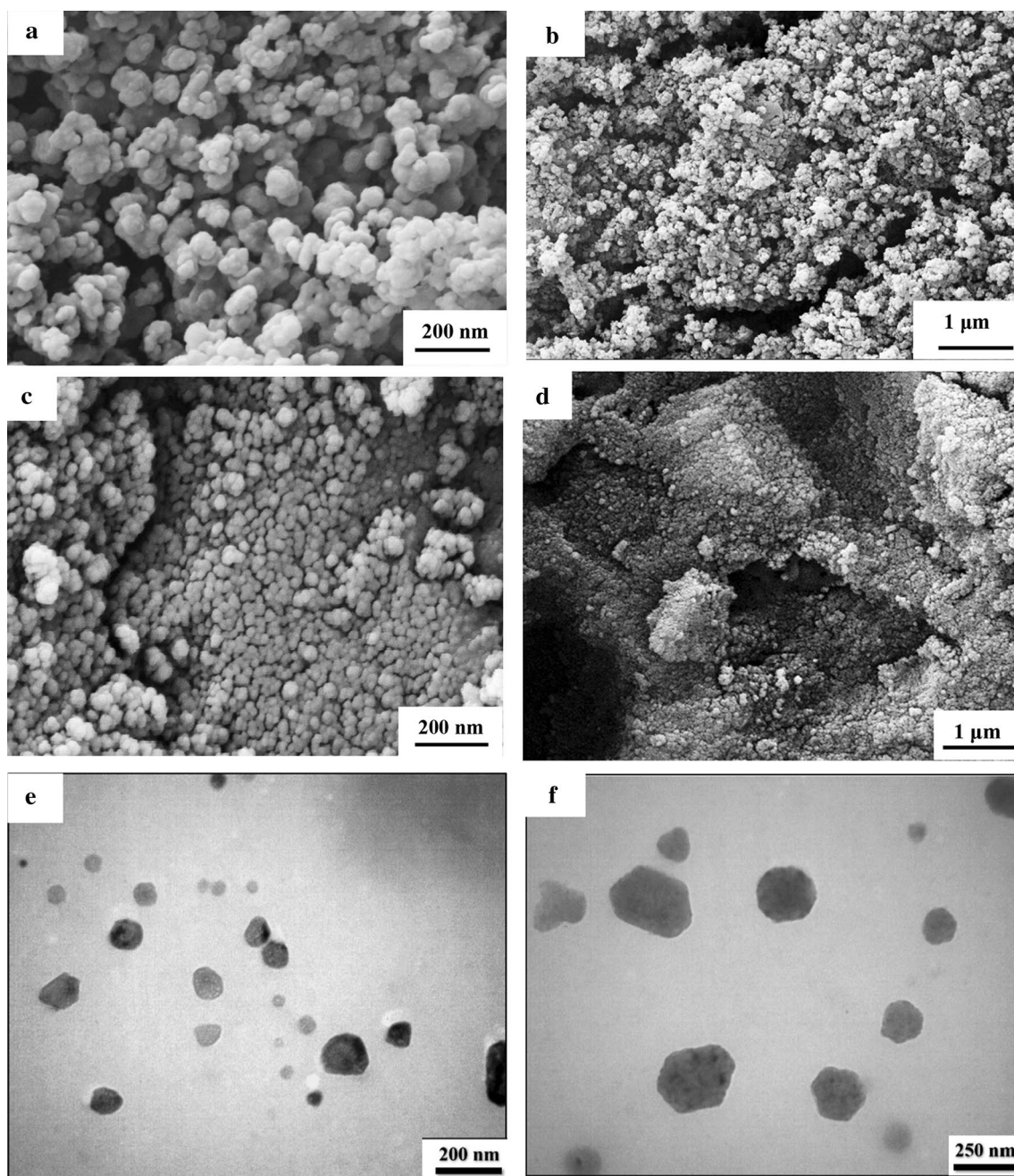


Fig. 3 FESEM images of CoFe_2O_4 @nano-Cell/ Fe (III) SSZ (**a**, **b**); CoFe_2O_4 Cell (**c**, **d**); TEM image of CoFe_2O_4 @nano-Cell/ Fe (III) SSZ and CoFe_2O_4 Cell (**e**, **f**)

Table 2 EDAX analysis of the catalysts

Entry	Substrate	C	N	O	S	Cl	Co	Fe
1	CoFe_2O_4 -Cell	19.3	0	15.0	0	4.6	2.7	37.4
2	Fe (III)-SSZ	38.5	9.4	21.2	9.1	11.6	0	10.2
3	CoFe_2O_4 Cell-Fe (III)/SSZ	39.9	15.5	16.2	2.0	0	4.1	22.3

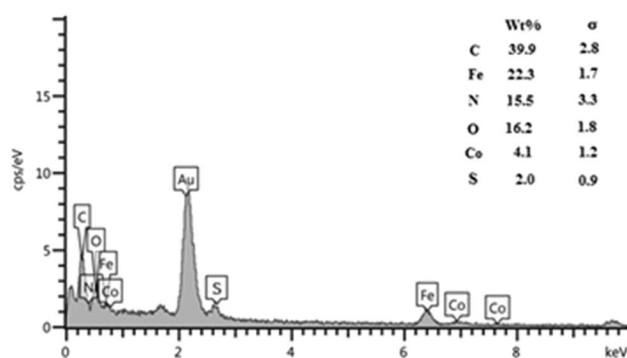


Fig. 4 EDAX spectra of CoFe_2O_4 -Cell/Fe (III)-SSZ

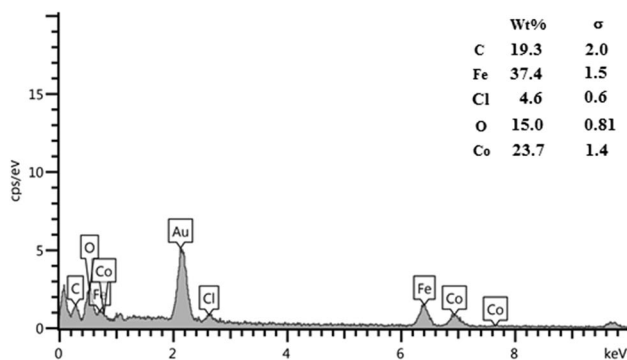


Fig. 5 EDAX spectra of CoFe_2O_4 Cell

Table 3 CHN analysis

Entry	Substrate	C	H	N
1	Cellulose	41.8	6.26	0
2	CoFe_2O_4 -Cell	20.8	4.67	0
3	SSZ	53.27	3.5	13.06
4	Fe (III)-SSZ	37.80	3.48	9.47
5	CoFe_2O_4 -Cell/Fe (III)-SSZ	26.3	4.64	2.87

the carboxylate group in the complex formation. The other ligand vibrations ($\text{O}=\text{S}$, $\text{O}=\text{N}$) remained unchanged or slightly shifted, which might be attributed to the electronic density changes on these groups after the complex formation. The participation of the phenolic and carboxylic groups was also confirmed by the appearance of a new signal in the complex in 440 cm^{-1} region assigned to the $\nu(\text{M}-\text{O})$ stretching vibrations [34]. The spectrum of CoFe_2O_4 -Cell/Fe (III) SSZ (Fig. 8e) showed sharp signals at 1604 and 1410 cm^{-1} related to asymmetric and symmetric stretching vibrations of the carboxylate group, respectively. This remarkable increase of frequency of the catalyst in comparison with ferric sulfasalazine indicated the participation

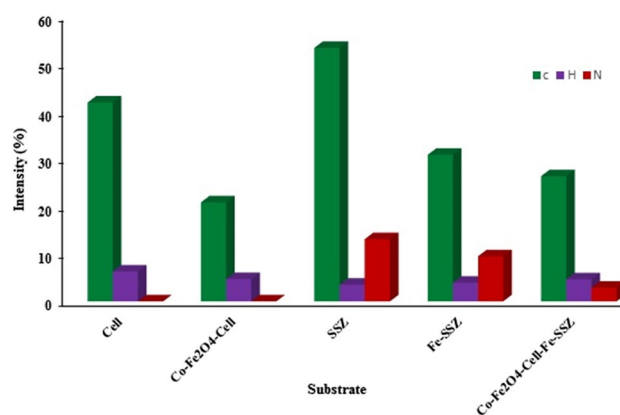


Fig. 6 CHN analysis of Cell, CoFe_2O_4 Cell, SSZ, Fe (III) SSZ and CoFe_2O_4 Cell-Fe (III) SSZ

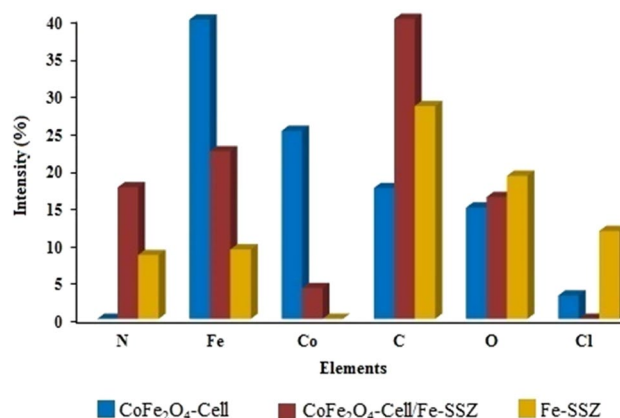


Fig. 7 EDAX analysis of CoFe_2O_4 , Fe (III) SSZ, CoFe_2O_4 Cell-Fe (III) SSZ

of the carboxylate group in the structure of the final catalyst. The sulfonyl group vibrations didn't show any changes obviously. Also a characteristic absorption band in 406 cm^{-1} could be due to Fe–O band for the ferric ion attached to cellulose [43, 44].

3.5 The Magnetic Properties

Magnetic properties of the magnetic properties of CoFe_2O_4 -cellulose and CoFe_2O_4 -cellulose/Fe (III)-SSZ were characterized at RT (300 K) by a vibrating sample magnetometer (VSM) and their hysteresis curves were presented in Fig. 9. The amount of specific saturation magnetization (M_s) for CoFe_2O_4 -cellulose nanoparticles was about 52.42 emu g^{-1} , which decreased to 37.40 emu g^{-1} after connecting ferric sulfasalazine to CoFe_2O_4 -cellulose. Although this noteworthy decrease, the saturated magnetization of the MNPs was sufficient for magnetic separation. Therefore

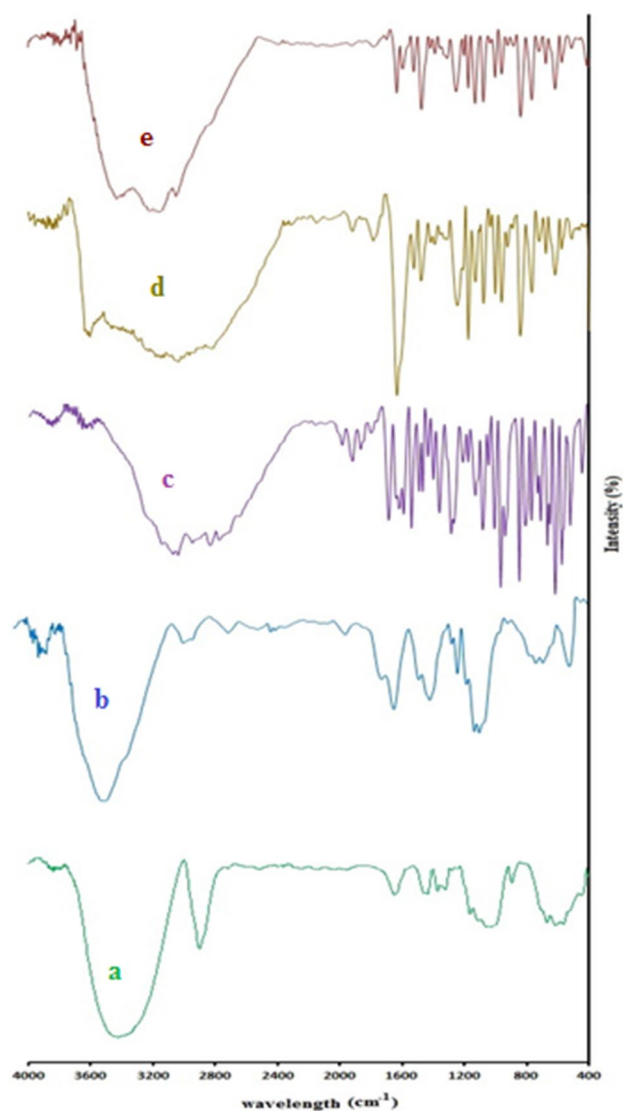


Fig. 8 FTIR of (a) cellulose (b) $\text{CoFe}_2\text{O}_4\text{Cell}$ (c) SSZ (d) Fe (III) SSZ (e) $\text{CoFe}_2\text{O}_4\text{@Cell-Fe (III) SSZ}$

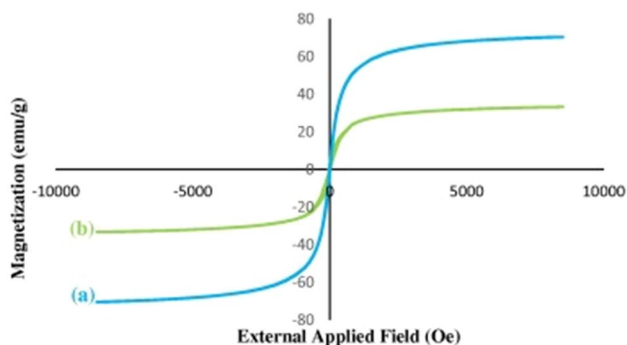


Fig. 9 Magnetization curves of (a) $\text{CoFe}_2\text{O}_4\text{Cell}$ (b) $\text{CoFe}_2\text{O}_4\text{@Cell-Fe (III) SSZ}$

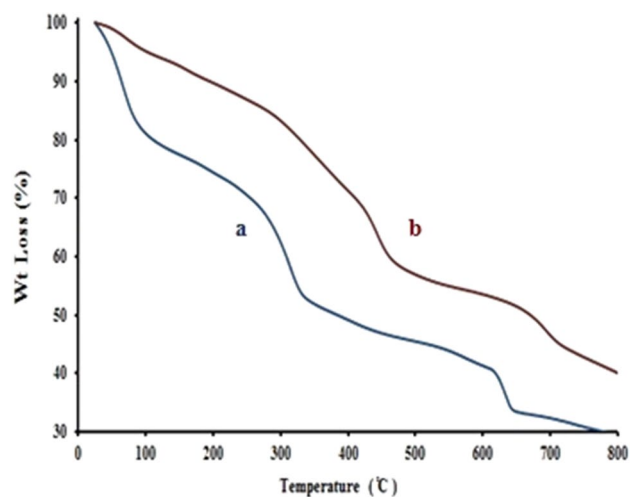


Fig. 10 TGA of (a) $\text{CoFe}_2\text{O}_4\text{Cell}$ (b) $\text{CoFe}_2\text{O}_4\text{@Cell-Fe (III) SSZ}$

the prepared catalyst could be separated efficiently via an external permanent magnet.

3.6 Thermogravimetric Studies

The TGA curve of $\text{CoFe}_2\text{O}_4\text{Cell}$ illustrated fourth mass-loss steps in Fig. 10a. The first one was a weight loss (18.2%) from 50 to 100 °C because of removal of catalyst moisture. The second step was the decomposition step with an estimated mass loss of 25.1% in the temperature range of 100–310 °C, due to the liberation of two coordinated water molecules. Consequently, the third weight loss in the series of 310–610 °C (10.1%) was related to the decomposition of cellulose units through the formation of levoglucosan and other volatile compounds. The fourth step with a final oxide residue of Fe_2O_3 and CoO (12.05%) was from 610 to 800 °C. Also the TGA curve of $\text{CoFe}_2\text{O}_4\text{Cell/Fe (III)-SSZ}$ illustrated five mass-loss steps in Fig. 10b. The first one, a very small weight loss (2.53%) from 50 to 100 °C was related to removal of catalyst moisture. The second step, the decomposition step with an estimated mass loss of 14.16% within the temperature range of 100 °C to 300 °C might be attributed to the liberation of two coordinated water molecules. Consequently, the third main weight loss observed in the in the ranges of 300–465 °C (24.10%) was due to the decomposition of cellulose units through the formation of levoglucosan and other volatile compounds. The fourth step from 465 to 645 °C with an estimated mass loss of 8.08% was considered to the decomposition of the ligand molecule. It ended at the fifth step with a final oxide residue of Fe_2O_3 and CoO (12.05%) with the range of 465–800 °C. Finally, based on the TGA curve, the stability of $\text{CoFe}_2\text{O}_4\text{Cell/Fe (III)-SSZ}$ was increased compared to $\text{CoFe}_2\text{O}_4\text{Cell}$.

3.7 Catalytic Activity of CoFe₂O₄-Cell-Fe (III)/ SSZ for 4H-Pyrans Synthesis

In order to evaluate the catalytic activity of ferric sulfa drug complex supported on CoFe₂O₄Cell, one-pot synthesis of malonitrile, aldehyde (or isatin) and ethyl acetoacetate (methyl acetoacetate and acetoacetone) was chosen. Benzaldehyde and ethyl acetoacetate were selected as the model compounds for the optimization of 4H-pyrans synthesis. The time and yield of the reaction catalyzed by CoFe₂O₄Cell/ Fe (III) SSZ were compared to other catalysts in Table 4. The reaction mostly was carried out successfully by strong basic catalysts. So the present catalyst as a heterogeneous acidic catalyst improved the yield under mild conditions. The reported catalysts such as decaniobate salt [16] was a homogeneous catalyst, which means it has no ability to be recovered. Also the reaction was carried out at high temperature during 120 min. Chitosan-grafted-poly (4-Vinylpyridine) [21] as a heterogeneous basic catalyst offered the product at reflux conditions after 180 min. Besides, the reaction was catalyzed by piperazine hydrate [21] and L- prolin [12] as homogeneous catalysts, suffered from high temperature and long reaction time. Although, the reaction was catalyzed by ammonium acetate [45] was carried at room temperature, but high catalyst loading applied (Table 4, entries 1–5). In the present research, α -Fe₂O₃, FeCl₃·6H₂O, CoCl₂·6H₂O, cellulose and CoFe₂O₄Cell were also applied as acidic base catalysts (Table 4, entries 6–10). Noticeably, CoFe₂O₄Cell improved the yield and decreased the reaction time compared to them. Furthermore, ferric sulfasalazine and ferric complex of salicylic acid (Table 4, entries 11 and 12) as organometallic catalysts displayed different results. Somehow, ferric sulfasalazine enhanced the yield to 78% in

a short time, but Fe (III)-SSA exhibited a poor yield in a long reaction time. Finally by attaching ferric sulfasalazine on super magnetic cellulose, the yield of the reaction was increased to 98% during 10 min. Furthermore the other features of CoFe₂O₄@Cell/ Fe (III) SSZ were: decreasing of the temperature to 60 °C and reusability (Table 4, entry 13).

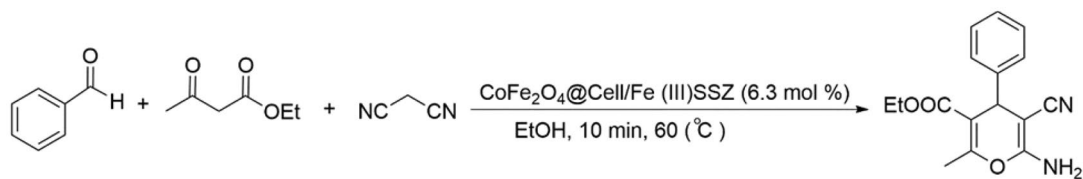
3.8 Optimization of the Reaction Conditions for the Synthesis of 4H- Pyrans

The temperature of the reaction from room temperature to 70 °C was studied (Table 5, entries 1–8). By applying the catalyst at room temperature, 70% of product was obtained during 100 min (Table 5, entry 1). Increasing the temperature from 40 to 55 °C improved production up to 90% obviously (Table 5, entries 2–5). The best result was obtained at 60 °C, in which the yield was enhanced to 98% (Table 5, entry 6). When the reaction was carried out at 65 °C, the corresponding yield didn't change (Table 5, entry 7). Conversion of the starting materials to the product at 70 °C decreased the yield to 95% (Table 5, entry 8).

Loading of the catalyst from 0 to 0.25 mol % was summarized in Table 5 (entries 9–15). The reaction was carried out without catalyst, somehow, after 720 min no product was obtained (Table 5, entry 9). Loading of the catalyst from 0.02 to 0.12 mol% increased production from 40 to 80% (Table 5, entries 10–12). Also the reaction time was decreased from 40 to 15 min by adding amount of the catalyst (Table 5, entries 10–12). When 0.16 mol% of the catalyst was consumed, the related production was increased to 98% (Table 5, entry 13). It was noticeable that addition of catalyst loading to 0.2 mol% and 0.25 mol% didn't change the yield (Table 5, entry 14–15).

Table 4 Optimization of catalyst for 4H- pyrans reaction

Entry	Catalyst	Solvent	Catalyst amount	Temperature (°C)	Time (min)	Yield (%)	References
1	HPNb	Solvent free	100 mg	80	120	91	Sarnikar et al. [32]
2	Cs-PVP	Absolute ethanol	10 wt%	Reflux	180	90	Shukla et al. [33]
3	Piperazine hydrate	EtOH	7 mol%	Reflux	540	85	Soliman et al. [34]
4	L-proline	EtOH	10 mol%	Reflux	240	72	Tamadon and Moradi [35]
5	NH ₄ OAC	EtOH	150 mol%	rt	720	78	Valkenber and Hölderich [36]
6	α -Fe ₂ O ₃	EtOH	0.01 g	60	30	69	Present
7	FeCl ₃ ·6H ₂ O	EtOH	0.01 g	60	720	20	Present
8	CoCl ₂ ·6H ₂ O	EtOH	0.01 g	60	720	23	Present
9	Cellulose	EtOH	0.01 g	60	90	80	Present
10	CoFe ₂ O ₄ -Cell	EtOH	0.01 g	60	30	85	Present
11	Fe (III)-SSZ	EtOH	0.01 g	60	30	78	Present
12	Fe (III)-SSA	EtOH	0.01 g	60	720	35	Present
13	CoFe ₂ O ₄ -Cell/Fe (III) SSZ	EtOH	0.01 g	60	10	98	Present

Table 5 Optimization of 4H- pyrans reaction


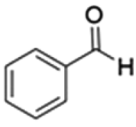
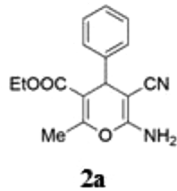
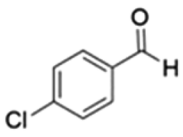
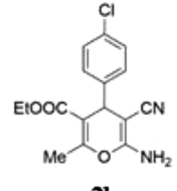
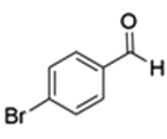
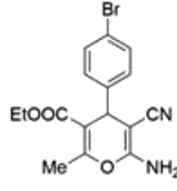
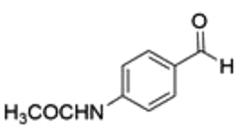
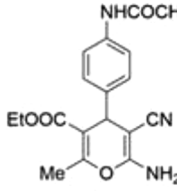
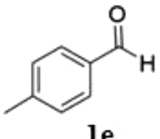
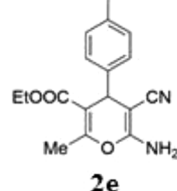
Entry	Catalyst	Solvent	X (mol%)	Temperature (°C)	Time (min)	Yield (%)
<i>Effect of temperature</i>						
1	CoFe ₂ O ₄ -Cell/Fe (III) SSZ	EtOH	0.16	rt	100	70
2	CoFe ₂ O ₄ -Cell/Fe (III) SSZ	EtOH	0.16	40	100	76
3	CoFe ₂ O ₄ -Cell/Fe (III) SSZ	EtOH	0.16	45	80	79
4	CoFe ₂ O ₄ -Cell/Fe (III) SSZ	EtOH	0.16	50	40	85
5	CoFe ₂ O ₄ -Cell/Fe (III) SSZ	EtOH	0.16	55	20	90
6	CoFe ₂ O ₄ -Cell/Fe (III) SSZ	EtOH	0.16	60	10	98
7	CoFe ₂ O ₄ -Cell/Fe (III) SSZ	EtOH	0.16	65	10	98
8	CoFe ₂ O ₄ -Cell/Fe (III) SSZ	EtOH	0.16	70	10	95
<i>Effect of catalyst loading</i>						
9	CoFe ₂ O ₄ -Cell/Fe (III) SSZ	EtOH	0	60	720	NR
10	CoFe ₂ O ₄ -Cell/Fe (III) SSZ	EtOH	0.02	60	40	40
11	CoFe ₂ O ₄ -Cell/Fe (III) SSZ	EtOH	0.07	60	30	60
12	CoFe ₂ O ₄ -Cell/Fe (III) SSZ	EtOH	0.12	60	15	80
13	CoFe ₂ O ₄ -Cell/Fe (III) SSZ	EtOH	0.16	60	10	98
14	CoFe ₂ O ₄ -Cell/Fe (III) SSZ	EtOH	0.2	60	10	98
15	CoFe ₂ O ₄ -Cell/Fe (III) SSZ	EtOH	0.25	60	10	98
<i>Effect of solvent</i>						
16	CoFe ₂ O ₄ -Cell/Fe (III) SSZ	EtOH	0.16	60	10	98
17	CoFe ₂ O ₄ -Cell/Fe (III) SSZ	EtOH/H ₂ O, (1:1)	0.16	60	15	75
18	CoFe ₂ O ₄ -Cell/Fe (III) SSZ	H ₂ O	0.16	60	20	35
19	CoFe ₂ O ₄ -Cell/Fe (III) SSZ	MeOH	0.16	60	10	90
20	CoFe ₂ O ₄ -Cell/Fe (III) SSZ	THF	0.16	60	60	27
21	CoFe ₂ O ₄ -Cell/Fe (III) SSZ	Toluene	0.16	60	120	23
22	CoFe ₂ O ₄ -Cell/Fe (III) SSZ	Solvent free	0.16	60	15	53
23	CoFe ₂ O ₄ -Cell/Fe (III) SSZ	DMF	0.16	60	14	71

The effect of solvents on the reaction was studied in Table 5 (entries 16–23). Ethanol as a green solvent was applied and increased the yield remarkably. Adding water to ethanol decreased the yield from 98 to 75% (Table 5, entry 17). Also applying water in the reaction resulted poor yield (Table 5, entry 18). Methanol as another alcohol was consumed and the related yield was 90%. Tetrahydrofuran, toluene and dimethylformamide as aprotic solvents didn't increase the production as much as alcohols (Table 5, entries 20, 21 and 23). It is worth mentioning that the reaction was carried out in solvent free conditions, but it didn't enhanced the yield noticeably (Table 5, entry 22).

3.9 Preparation of Functionalized 4H- Pyrans in the Presence of CoFe₂O₄@Cell/Fe (III)-SSZ

After optimization of the reaction conditions, the generality and scope of the reaction were considered. A diversity of aromatic aldehydes bearing electron donating and electron withdrawing groups at either ortho-, meta- or para-positions of the aromatic ring were transformed to 2-amino-4H-pyran derivatives with excellent yields (Table 6). An extensive range of useful functional groups including halide, nitro and isatin stayed stable during the reaction conditions (Table 6, entries 2, 6 and 13). In addition, the presence of amide, methyl and methoxy as

Table 6 Derivatives of 4-H pyrans

Entry	Substrate	1,3-Dicarbonyl	Product	Time (min)	Yield (%)
1	 1a	MeCO ₂ Et	 2a	10	98
2	 1b	MeCO ₂ Et	 2b	8	98
3	 1c	MeCO ₂ Et	 2c	9	97
4	 1d	MeCO ₂ Et	 2d	15	90
5	 1e	MeCO ₂ Et	 2e	11	91

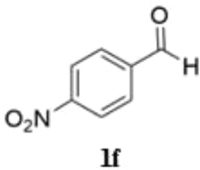
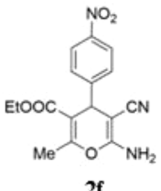
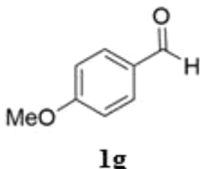
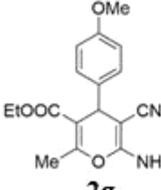
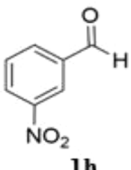
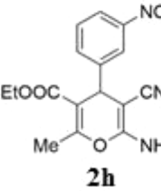
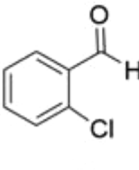
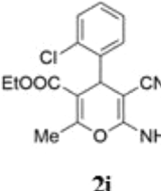
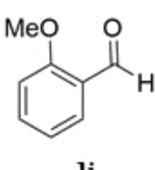
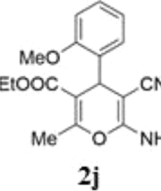
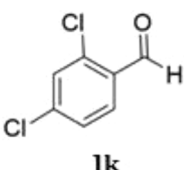
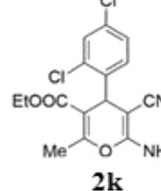
electron donating groups on the aromatic aldehyde performed well and offered the desired products up to 90% (Table 6, entries 4, 5 and 10). Furthermore, heterocycle groups such as furan and thiophene were successfully converted into the desired products with high yields (Table 6, entries 14 and 15). 5-Chloroisatin with an electron withdrawing group offered the related 4H-pyran with 98% yield after 10 min (Table 6, entry 13). Furthermore, methyl acetoacetate (Table 6, entries 23–25) had similar results as ethyl acetoacetate. It is noticeable, the reaction time

was decreased slightly by applying acetoacetone (Table 6, entries 18–22). This could be due to more activity of acetoacetone compared to ethyl acetoacetate (or methyl acetoacetate).

3.10 Recycling of the Catalyst

The magnetic property of CoFe₂O₄@Cell/Fe (III)-SSZ caused an efficient recovery of the catalyst from the reaction mixture. After completion of the reaction, the catalyst

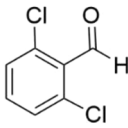
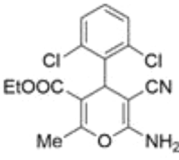
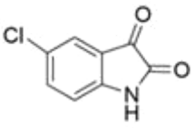
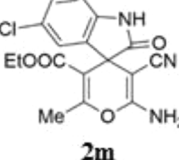
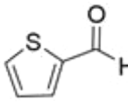
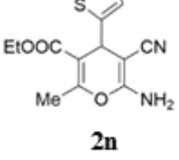
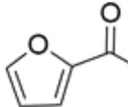
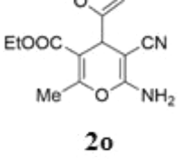
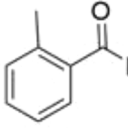
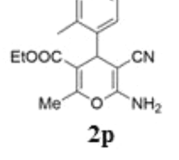
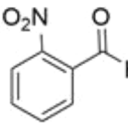
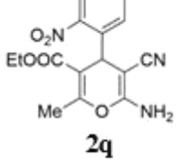
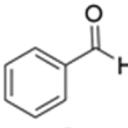
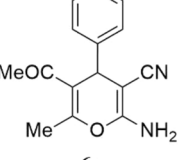
Table 6 (continued)

6	 <p>1f</p>	MeCO ₂ Et	 <p>2f</p>	8	95
7	 <p>1g</p>	MeCO ₂ Et	 <p>2g</p>	13	90
8	 <p>1h</p>	MeCO ₂ Et	 <p>2h</p>	10	97
9	 <p>1i</p>	MeCO ₂ Et	 <p>2i</p>	10	96
10	 <p>1j</p>	MeCO ₂ Et	 <p>2j</p>	10	94
11	 <p>1k</p>	MeCO ₂ Et	 <p>2k</p>	9	96

was separated by a strong external permanent magnet, washed with ethanol, dried under vacuum, and reused directly for another run. The catalyst was consumed with sixth runs, and no significant loss of catalytic activity was

observed (Fig. 11). FT-IR and SEM images of fresh and recovered catalysts indicated that no considerable change didn't occur (Figs. 12, 13). This showed that CoFe₂O₄@Cell/Fe (III)-SSZ is a stable chemical compound.

Table 6 (continued)

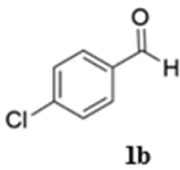
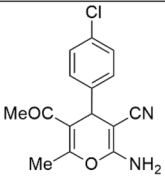
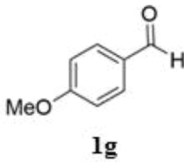
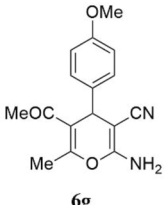
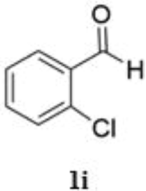
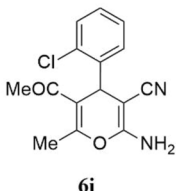
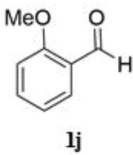
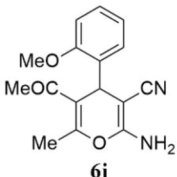
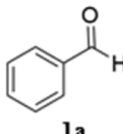
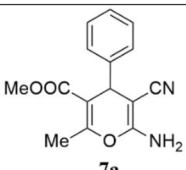
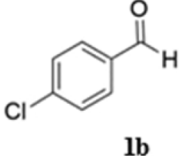
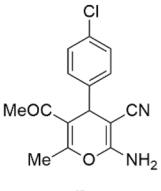
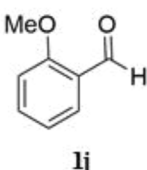
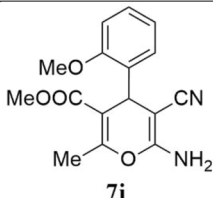
12	 11	MeCO ₂ Et	 21	9	93
13	 1m	MeCO ₂ Et	 2m	10	98
14	 1n	MeCO ₂ Et	 2n	14	90
15	 1o	MeCO ₂ Et	 2o	13	92
16	 1p	MeCO ₂ Et	 2p	11	90
17	 1q	MeCO ₂ Et	 2q	10	93
18	 1a	MeCOCH ₂ COMe	 6a	9	96

3.11 Optimization of the Reaction Conditions for the Synthesis of 1,4-DHP

In order to compare the efficiency of the nano catalyst, the model reaction was carried out in the presence of various

catalysts (as indicated in Table 7). Silica gel/sulfonic acid [15] as a heterogeneous catalyst needed high catalyst loading and long reaction time. Also, *p*-toluene sulfuric acid [20] catalyzed the reaction via ultrasonic irradiation. This homogeneous catalyst didn't reduce the reaction time obviously.

Table 6 (continued)

19	 <p>1b</p>	MeCOCH ₂ COMe	 <p>6b</p>	8	97
20	 <p>1g</p>	MeCOCH ₂ COMe	 <p>6g</p>	11	93
21	 <p>1i</p>	MeCOCH ₂ COMe	 <p>6i</p>	9	94
22	 <p>1j</p>	MeCOCH ₂ COMe	 <p>6j</p>	10	92
23	 <p>1a</p>	MeCO ₂ Me	 <p>7a</p>	10	95
24	 <p>1b</p>	MeCO ₂ Me	 <p>6b</p>	9	97
25	 <p>1j</p>	MeCO ₂ Me	 <p>7j</p>	12	91

Furthermore, samarium (III) chloride [32] as another homogeneous catalyst was not able to be reused. In addition, the reaction needed long time and high catalyst loading. PdRuNi

supported on graphene oxide [9] catalyzed the reaction in DMF, which is not a green solvent. However, the loading of the catalyst was low, but the catalyst is expensive

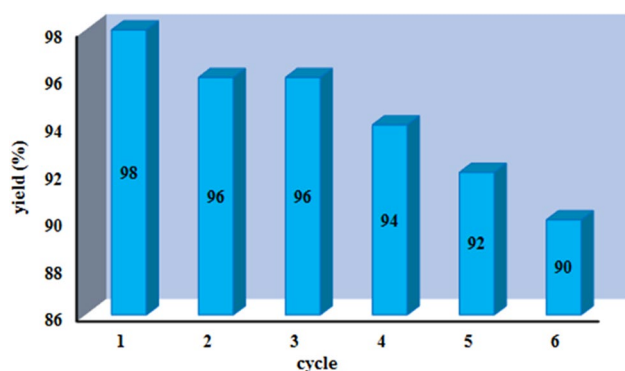


Fig. 11 Recyclability of the catalyst for the 4-H pyran synthesis

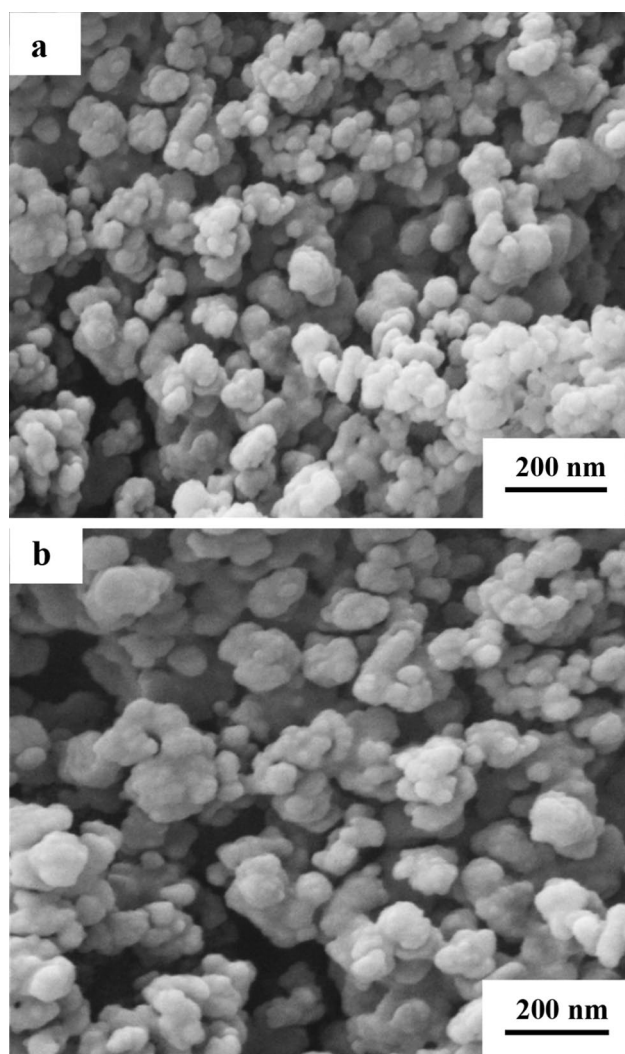


Fig. 12 SEM images of **a** Fresh $\text{CoFe}_2\text{O}_4@\text{Cell}/\text{Fe (III) SSZ}$ and **b** $\text{CoFe}_2\text{O}_4@\text{Cell}/\text{Fe (III) SSZ}$ after three runs

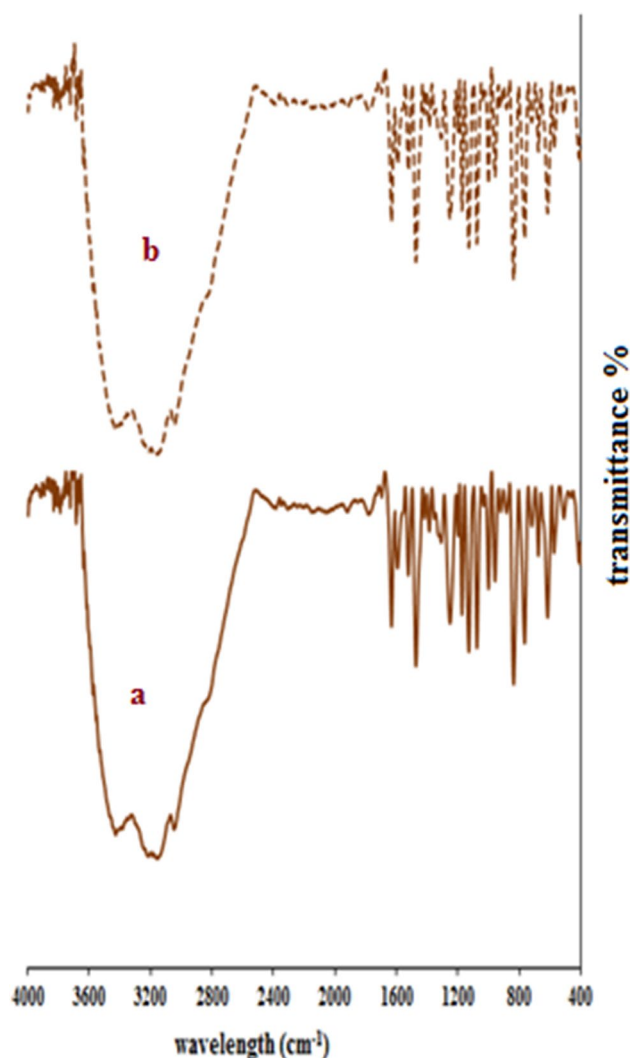


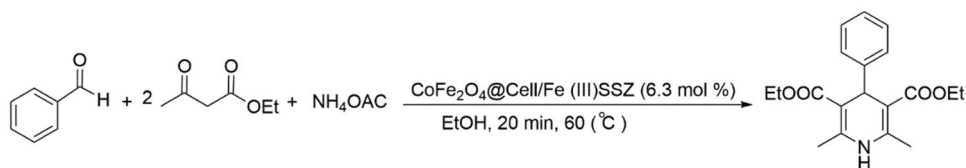
Fig. 13 FT-IR spectra of (a) Fresh $\text{CoFe}_2\text{O}_4@\text{Cell}/\text{Fe (III) SSZ}$ and (b) $\text{CoFe}_2\text{O}_4@\text{Cell}/\text{Fe (III) SSZ}$ after three runs

and it didn't reduce the reaction time noticeably (Table 7, entries 1–4). In this research, cellulose, $\text{FeCl}_3 \cdot 6\text{H}_2\text{O}$ and $\text{CoCl}_2 \cdot 6\text{H}_2\text{O}$ (Table 7, entries 5–7) were applied as catalysts. They all needed longer reaction time compared to $\text{CoFe}_2\text{O}_4\text{Cell}$ at 60°C (Table 7, entry 8) which reduced the reaction time to 30 min. Besides, ferric sulfasalazine and ferric salicylic acid were used in which both required more reaction time than $\text{CoFe}_2\text{O}_4\text{Cell}$ (Table 7, entries 9 and 10). Although Fe (III)-SSZ displayed more activity than Fe (III) SSA. Finally $\text{CoFe}_2\text{O}_4@\text{Cell}/\text{Fe (III) SSZ}$ catalyzed the reaction successfully during 20 min with 97% yield (Table 7, entry 11).

Optimization of temperature, catalyst loading and solvent of the reaction was summarized in Table 8. The effect of the temperature was traced, and the reaction was carried out from room temperature to 70°C (Table 8, entries 1–5). The highest yield was obtained at 60°C (Table 8,

Table 7 Optimization of catalyst for 1,4-DHP synthesis

Entry	Catalyst	Solvent	Catalyst amount	Temperature (°C)	Time (min)	Yield (%)	References
1	SiO ₂ -SO ₃ H	Solvent free	0.2 g	60	330	90	Zhao et al. [43]
2	<i>p</i> -TSA	EtOH	10 mol %	Ultrasonic irradiation	60	78	Zhao et al. [44]
3	SmCl ₃	CH ₃ CN	20 mol %	70	180	85	Zonouz et al. [45]
4	PdNiRu@GO	DMF	0.006 g	70	45	93	Demirci et al. [9]
5	Cellulose	EtOH	0.01 g	60	300	41	Present
6	FeCl ₃ .6H ₂ O	EtOH	0.01 g	60	120	30	Present
7	CoCl ₂ .6H ₂ O	EtOH	0.01 g	60	120	32	Present
8	CoFe ₂ O ₄ Cell	EtOH	0.01 g	60	30	79	Present
9	Fe (III) SSZ	EtOH	0.01 g	60	35	56	Present
10	Fe (III) SSA	EtOH	0.01 g	60	45	40	Present
11	CoFe ₂ O ₄ -Cell/Fe (III) SSZ	EtOH	0.01 g	60	20	97	Present

Table 8 Optimization of 1,4-DHP synthesis


Entry	Catalyst	Solvent	X (mol%)	Temperature (°C)	Time (min)	Yield (%)
<i>Effect of temperature</i>						
1	CoFe ₂ O ₄ -Cell/Fe (III) SSZ	EtOH	0.16	rt	50	50
2	CoFe ₂ O ₄ -Cell/Fe (III) SSZ ₂	EtOH	0.16	40	40	59
3	CoFe ₂ O ₄ -Cell/Fe (III) SSZ	EtOH	0.16	50	30	69
4	CoFe ₂ O ₄ -Cell/Fe (III) SSZ	EtOH	0.16	60	20	97
5	CoFe ₂ O ₄ -Cell/Fe (III) SSZ	EtOH	0.16	70	20	97
<i>Effect of catalyst loading</i>						
6	CoFe ₂ O ₄ -Cell/Fe (III) SSZ	EtOH	0	60	240	15
7	CoFe ₂ O ₄ -Cell/Fe (III) SSZ	EtOH	0.02	60	45	71
8	CoFe ₂ O ₄ -Cell/Fe (III) SSZ	EtOH	0.125	60	30	86
9	CoFe ₂ O ₄ -Cell/Fe (III) SSZ	EtOH	0.16	60	20	97
10	CoFe ₂ O ₄ -Cell/Fe (III) SSZ	EtOH	0.2	60	20	97
11	CoFe ₂ O ₄ -Cell/Fe (III) SSZ	EtOH	0.25	60	20	97
<i>Effect of solvent</i>						
12	CoFe ₂ O ₄ -Cell/Fe (III) SSZ	EtOH	0.16	60	20	97
13	CoFe ₂ O ₄ -Cell/Fe (III) SSZ	EtOH/H ₂ O, (1:1)	0.16	60	30	70
14	CoFe ₂ O ₄ -Cell/Fe (III) SSZ	H ₂ O	0.16	60	30	36
15	CoFe ₂ O ₄ -Cell/Fe (III) SSZ	MeOH	0.16	60	20	89
16	CoFe ₂ O ₄ -Cell/Fe (III) SSZ	THF	0.16	60	60	29
17	CoFe ₂ O ₄ -Cell/Fe (III) SSZ	Toluene	0.16	60	120	33
18	CoFe ₂ O ₄ -Cell/Fe (III) SSZ	Solvent free	0.16	60	20	63
19	CoFe ₂ O ₄ -Cell/Fe (III) SSZ	DMF	0.16	60	25	74

entry 4). Furthermore the reaction yield didn't change by increasing the temperature (Table 8, entry 5). It is worth mentioning that loading of the catalyst from 0 to

0.25 mol% was summarized in Table 8 (entries 6–11), somehow the best result occurred by loading 0.16 mol% of the catalyst (Table 8, entry 9). It is notable that the yield

Table 9 Synthesis of 1,4-DHP derivatives

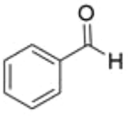
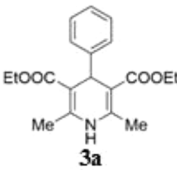
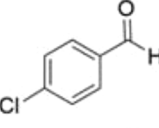
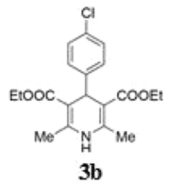
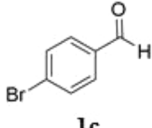
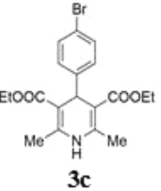
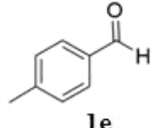
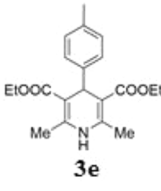
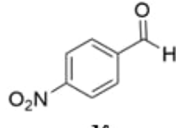
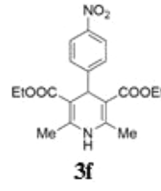
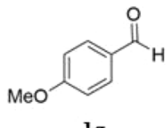
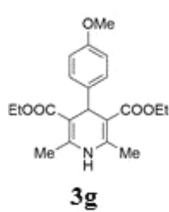
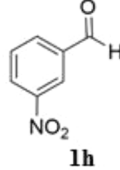
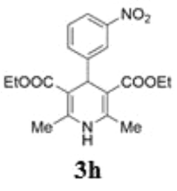
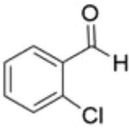
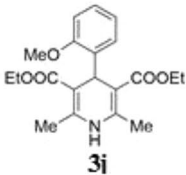
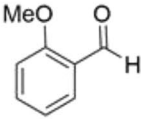
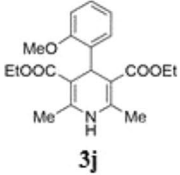
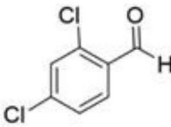
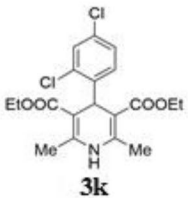
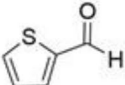
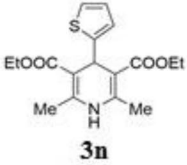
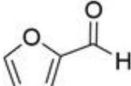
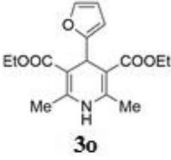
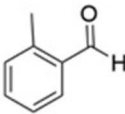
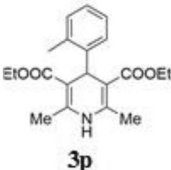
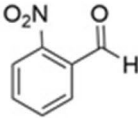
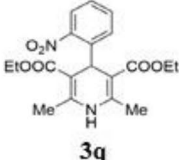
Entry	Substrate	1,3-Dicarbonyl	Product	Time (min)	Yield (%)
1	 1a	MeCO ₂ Et	 3a	20	97
2	 1b	MeCO ₂ Et	 3b	18	96
3	 1c	MeCO ₂ Et	 3c	19	93
4	 1e	MeCO ₂ Et	 3e	20	90
5	 1f	MeCO ₂ Et	 3f	18	97
6	 1g	MeCO ₂ Et	 3g	20	90
7	 1h	MeCO ₂ Et	 3h	19	96

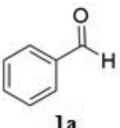
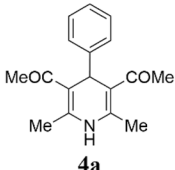
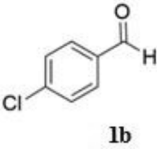
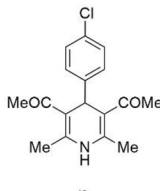
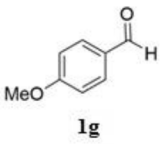
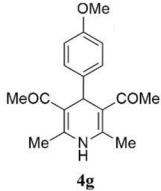
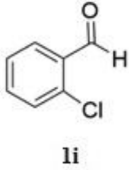
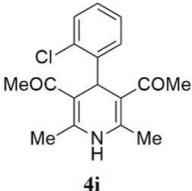
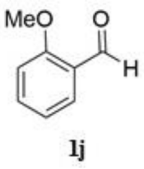
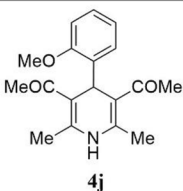
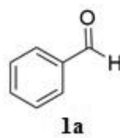
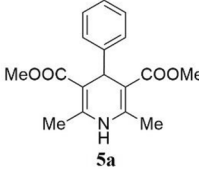
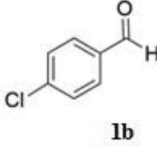
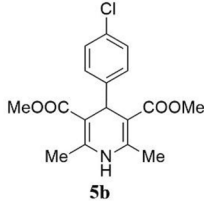
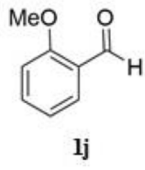
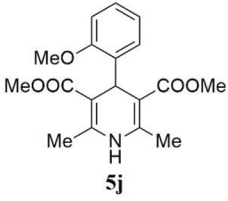
Table 9 (continued)

8	 1i	MeCO ₂ Et	 3j	19	93
9	 1j	MeCO ₂ Et	 3j	20	90
10	 1k	MeCO ₂ Et	 3k	19	96
11	 1n	MeCO ₂ Et	 3n	20	95
12	 1o	MeCO ₂ Et	 3o	20	92
13	 1p	MeCO ₂ Et	 3p	20	90
14	 1q	MeCO ₂ Et	 3q	20	97

didn't improve by increasing the amount of catalyst from 0.16 mol% to 0.2 and 0.25 mol% (Table 8, entries 10 and 11). Ethanol (Table 8, entry 12) was an appropriate and green solvent between aprotic and protic solvents (Table 8,

entry 12–19). The production of 1, 4-DHP was decreased by adding water as a solvent (Table 8, entries 13 and 14). Also solvent free solvent conditions didn't improve the yield considerably (Table 8, entry 18).

Table 9 (continued)

15	 1a	MeCOCH ₂ COMe	 4a	19	93
16	 1b	MeCOCH ₂ COMe	 4b	18	95
17	 1g	MeCOCH ₂ COMe	 4g	20	90
18	 1i	MeCOCH ₂ COMe	 4i	19	95
19	 1j	MeCOCH ₂ COMe	 4j	20	90
20	 1a	MeCO ₂ Me	 5a	20	90
21	 1b	MeCO ₂ Me	 5b	19	92
22	 1j	MeCO ₂ Me	 5j	20	90

3.12 Preparation of Functionalized 1,4-DHP Derivatives in the Presence of $\text{CoFe}_2\text{O}_4\text{@Cell/Fe (III)-SSZ}$

After optimization of the reaction conditions, the generality and scope of the reaction were considered. As demonstrated in Table 9, a diversity of aromatic aldehydes bearing electron donating and electron withdrawing groups at either ortho-, meta- or para-positions of the aromatic ring were transformed to 1,4-dihydropyridines derivatives with excellent yields under mild conditions. A wide variety of synthetically useful functional groups including halide and nitro stayed undamaged during the reaction conditions. Furthermore, the presence of methoxy, methyl as electron donating groups on the aromatic aldehyde performed well and offered the product up to 90% yield. Also, heterocycle groups such as furan and thiophene were successfully converted into the desired products in high yield (Table 9, entries 11 and 12). Furthermore the related products were obtained with high yields by applying acetoacetone (Table 9, entries 15–19) and methyl acetoacetate (Table 9, entries 20–22). Methyl acetoacetate offered the desired products almost same as ethyl acetoacetate. However, acetoacetone could reduce the time of reaction a little. This

might be because of its higher activity compared to ethyl acetoacetate (or methyl acetoacetate).

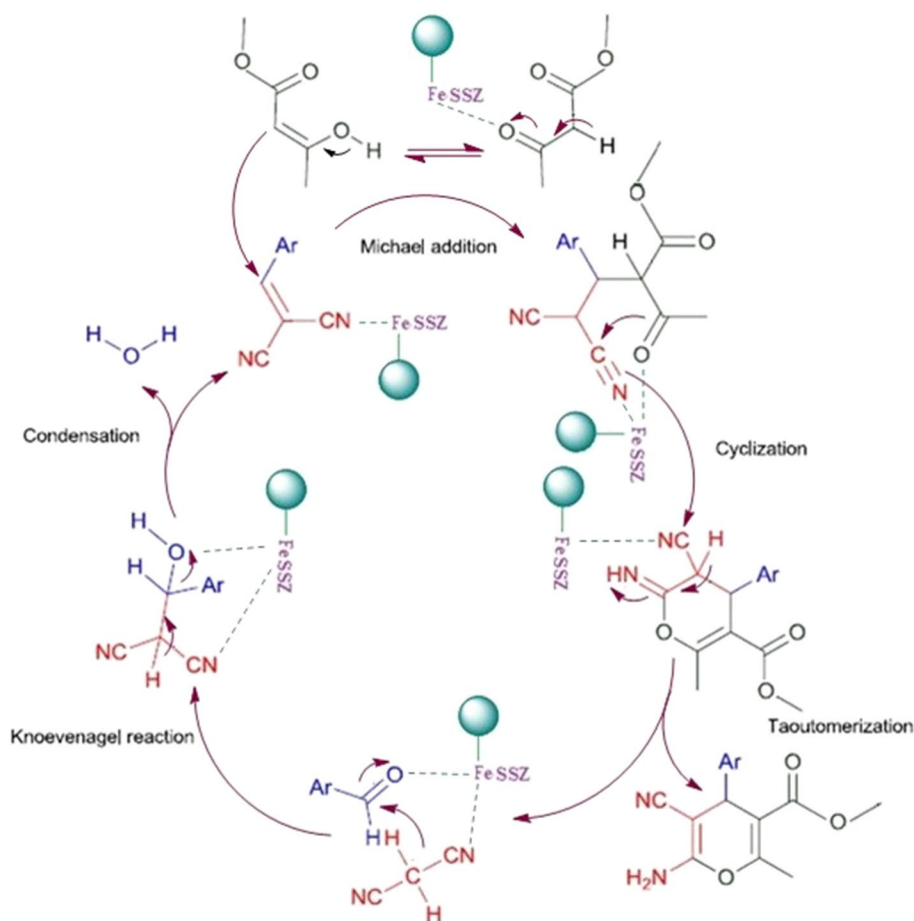
3.12.1 Proposed Mechanism of $\text{CoFe}_2\text{O}_4\text{@Cell/Fe (III)-SSZ}$ Catalyzed 4H-Pyran Synthesis

The mechanism of 4H-pyran synthesis catalyzed by $\text{CoFe}_2\text{O}_4\text{@Cell/Fe (III)-SSZ}$ was illustrated in Scheme 2. Ferric ion has ability to activate carbonyl and nitrogen groups. So, 2-benzylidenemalononitrile was formed immediately. Also 2-benzylidenemalononitrile and ethyl acetoacetate were catalyzed for Michael addition by connection to ferric ion through nitrogen and oxygen elements. After this step, cyclization occurred by enol addition to cyanide group (catalyzed both groups via the catalyst). Finally, 4-H pyran was produced after tautomerization. The catalyst was reused for the next run.

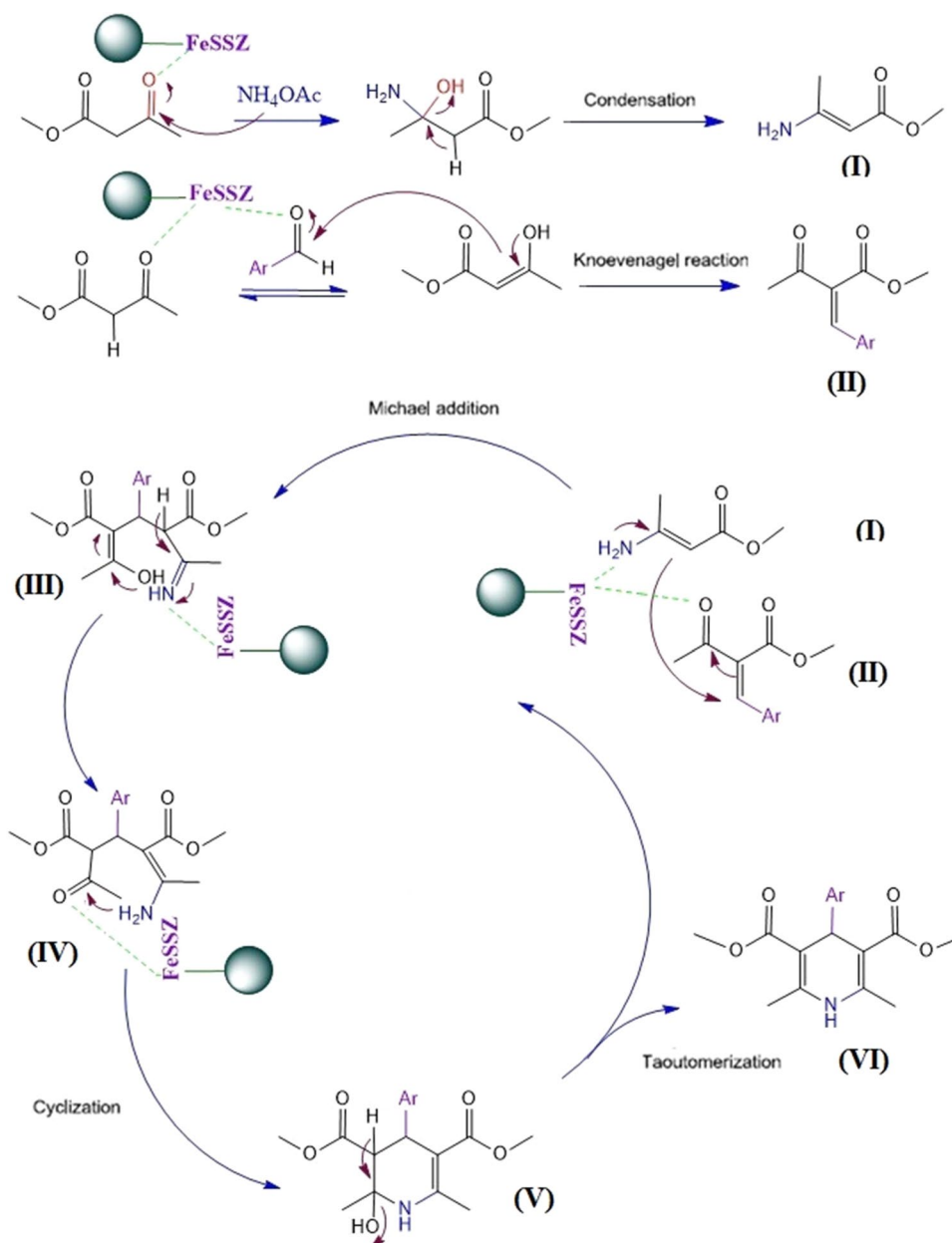
3.12.2 Suggested Mechanism of $\text{CoFe}_2\text{O}_4\text{@Cell/Fe (III)-SSZ}$ catalyzed 1,4-DHP Synthesis

The mechanism of preparation of 1, 4-DHP catalyzed by $\text{CoFe}_2\text{O}_4\text{@Cell/Fe (III)-SSZ}$ was demonstrated in Scheme 3. Firstly, intermediates of I and II were prepared by the

Scheme 2 The proposed mechanism of $\text{CoFe}_2\text{O}_4\text{@Cell-Fe (III) SSZ}$ for 4-H pyran synthesis



Scheme 3 The suggested mechanism of $\text{CoFe}_2\text{O}_4\text{Cell-Fe}$ (III) SSZ for 1, 4-DHP synthesis



heterogeneous catalyst. Ferric ion has ability to make carbonyl and nitrogen groups active. So, they reacted with each other via Michael addition. Consequently, intermediate of (III) was produced. After this step, cyclization was carried out by enamine addition to the carbonyl group (activated both groups through the catalyst). Tautomerization process offered 1, 4-DHP (VI). The catalyst was consumed again for the following run.

4 Conclusion

In summary, a nano sized magnetic $\text{CoFe}_2\text{O}_4\text{@Cell/Fe}$ (III)-SSZ was prepared and characterized by XRD, TEM, SEM, TGA, EDX, ICP-MS and IR spectroscopy. The catalyst

showed high activity for the one pot and atom-economical synthesis of 4H- pyrans and 1,4-DHP derivatives. This environmental heterogeneous organometallic catalyst proceeded the reactions under green conditions which offered products in high to excellent yields. Also the use of sulfasalazine for the first time as a pharmaceutical ligand in this organometallic catalyst was the novelty of research. Furthermore, ferric ion as a green, available and inexpensive metal and catalyst was consumed in the structure of sulfa drug complex. Besides, cellulose as a bio-friendly and bio-polymer support was applied. Magnetization of the catalyst was carried out by cobalt ferrite as one of the most versatile magnetic materials. It is worth mentioning, the catalyst readily was recovered by applying an external magnet. It was recycled

for several times without considerable loss of its catalytic activity. Finally the ability of the present catalyst with an important potential use for other multi component reactions is possible.

Acknowledgements The authors are thankful to Iran National Science Foundation (INSF) and K. N. Toosi University of Technology.

References

- Abdelrazek FM, Metz P, Kataeva O, Jager A, El-Mahrouky SF (2007) Synthesis and molluscicidal activity of new chromene and pyrano[2,3-c]pyrazole derivatives. *Arch der Pharm* 340(10):543–548. <https://doi.org/10.1002/ardp.200700157>
- Anastas PT, Kirchhoff MM (2002) Origins, current status, and future challenges of green chemistry. *Acc Chem Res* 35:686–694. <https://doi.org/10.1021/ar010065m>
- Azad S, Mirjalili BBF (2016) Fe_3O_4 @nano-cellulose/TiCl₄: a bio-based and magnetically recoverable nano-catalyst for the synthesis of pyrimido [2, 1-b] benzothiazole derivatives. *RSC Adv* 6:96928–96934. <https://doi.org/10.1039/C6RA13566H>
- Baig RBN, Varma RS (2013) Copper on chitosan: a recyclable heterogeneous catalyst for azide–alkyne cycloaddition reactions in water. *Green Chem* 15:398–417. <https://doi.org/10.1039/C3GC40401C>
- Bonsignore L, Loy G, Secci D, Calignano A (1993) Synthesis and pharmacological activity of 2-oxo-(2H) 1-benzopyran-3-carboxamide derivatives. *Eur J Med* 28(6):517–520
- Chen MN, Mo LP, Cui ZS, Zhang ZH (2019) Magnetic nano catalysts: synthesis and application in multicomponent reactions. *Curr Opin Green Sustain Chem* 15:27. <https://doi.org/10.1016/j.cogsc.2018.08.009>
- Chen HJ, Lin ZY, Li MY, Lian RJ, Xue QW, Chung JL, Chen SC, Chen YJ (2010) A new, efficient, and inexpensive copper (II)/salicylic acid complex catalyzed Sonogashira-type cross-coupling of haloarenes and iodoheteroarenes with terminal alkynes. *Tetrahedron* 66:7755–7761. <https://doi.org/10.1016/j.tet.2010.07.072>
- Cornils B, Herrmann, WA (1996) Applied homogeneous catalysis with organometallic compounds, Weinheim, Germany. A comprehensive handbook in three volumes, Weinheim, Germany. A comprehensive handbook in three volumes 1–2. ISBN: 978-3-527-30434-9.
- Demirci T, Çelik B, Yıldız Y, Eriş S, Arslan M, Sen F, Kilbas B (2016) One-pot synthesis of Hantzsch dihydropyridines using a highly efficient and stable PdRuNi@GO catalyst. *RSC Adv* 6:76948–76956. <https://doi.org/10.1039/C6RA13142E>
- Eddaoudi M, Moler DB, Li H, Chen B, Reineke TM, Keffe MO, Yaghi OM (2001) Modular chemistry: secondary building units as a basis for the design of highly porous and robust metal-organic carboxylate frameworks. *Acc Chem Res* 34:319. <https://doi.org/10.1021/ar000034b>
- Elnagdi HMN, Al-Hokbany SN (2012) Organocatalysis in synthesis: *L*-proline as an enantioselective catalyst in the synthesis of pyrans and thiopyrans. *Molecules* 17:4300–4312. <https://doi.org/10.3390/molecules17044300>
- Esfahani MN, Hoseini SJ, Montazerzohori M, Mehrabi R, Nasrabadi H (2014) Synthesis and characterization of magnetic bromochromate hybrid nanomaterials with triphenylphosphine surface-modified iron oxide nanoparticles and their catalytic application in multicomponent reactions. *J Mol Catal A* 382:99–105. <https://doi.org/10.1039/C4RA04654D>
- Gawande MB, Luque R, Zboril R (2014) The rise of magnetically recyclable nanocatalysts. *Chem Cat Chem* 6(12):3312–3313. <https://doi.org/10.1002/cctc.201402663>
- Green GR, Evans JM, Vong AK (1995) Pyrans and their benzo derivatives synthesis. In: Katritzky AR, Rees CW, Scriven EFV (eds) *Comprehensive heterocyclic chemistry II*, vol 5. Pergamon Press, Oxford, p 469
- Gupta R, Gupta R, Paul S, Loupy A (2007) Covalently anchored sulfonic acid on silica gel as an efficient and reusable heterogeneous catalyst for the one-pot synthesis of Hantzsch 1, 4-dihydropyridines under solvent-free conditions. *Synthesis* 18:2835–2838. <https://doi.org/10.1055/s-2007-983839>
- Gutierrez FL, Nope E, Rojas AH, Cubillos AJ, Sathicq GA, Romanelli PG, Martí'nez JJ, (2018) New application of decanobate salt as basic solid in the synthesis of 4H-pyrans by microwave assisted multicomponent reactions. *Res Chem Intermed* 44(9):5559–5568. <https://doi.org/10.1007/s11164-018-3440-y>
- Hou JT, Gao JW, Zhang ZH (2011) NbCl₅: an efficient catalyst for one-pot synthesis of α -amino phosphonates under solvent-free conditions. *Appl Organomet Chem* 25:47–53. <https://doi.org/10.1002/aoc.1687>
- Kaufman BM (2013) The American society of health-system pharmacists midyear clinical meeting & exhibition. *P&T* 38:119–120
- Khalil DK, Al-Matar MH (2013) Chitosan based heterogeneous catalyses: chitosan-grafted-poly (4-Vinylpyridine) as an efficient catalyst for Michael additions and alkyldiazinyl carbonitrile oxidation. *Molecules* 18:5288–5305. <https://doi.org/10.1080/17518253.2012.691183>
- Kumar A, Maurya RA (2008) Efficient synthesis of hantzsch esters and polyhydroquinoline derivatives in aqueous micelles. *Synlett* 6:883–885. <https://doi.org/10.1055/s-2008-1042908>
- Naghiyev F, Mamedov F, Khrustalev V, Shixaliyev N, Maharramov A (2009) A new direction in the alkylation of 5-acetyl-2-amino-6-methyl-4-phenyl-4H-pyran-3-carbonitrile with active methylene reagents. *J Chin Chem Soc* 50:4125–4127. <https://doi.org/10.1002/jccs.201800283>
- Noyori R (1994) *Asymmetric catalysis in organic synthesis*. Wiley, New York. ISBN: 978-0-471-57267-1
- Nurchi VM, Alonso MC, Toso L, Lachowicz JJ, Crisponi G, Alberti G, Biesur R, Martin AD, Gutierrez JN, Perez JMG, Zoroddu MA (2013) Iron (III) and aluminium (III) complexes with substituted salicyl-aldehydes and salicylic acids. *J Inorg Biochem* 128:174–182. <https://doi.org/10.1016/j.jinorgbio.2013.07.016>
- Nurchi VM, Pivetta T, Lachowicz JJ, Crisponi G (2009) Effect of substituents on complex stability aimed at designing new iron(III) and aluminum(III) chelators. *J Inorg Biochem* 103:227–236. <https://doi.org/10.1016/j.jinorgbio.2008.10.011>
- Praveen K, Madhavi DSS, Kumar KA, Kumar YK (2016) Microstructure and mechanical properties of MG/WC composites prepared by stir casting method. *Int J Eng Sci Invent* 5(9):8–10
- Pozdnyakov IP, Plyusnin VF, Grivin VP, Oliveros E (2015) Photochemistry of Fe (III) and sulfosalicylic acid aqueous solutions. *J Photochem Photobiol A* 307–308:9–15. <https://doi.org/10.1016/j.jphotochem.2006.01.017>
- Rajput JK, Kaur G (2014) Synthesis and applications of CoFe₂O₄ nanoparticles for multicomponent reactions. *Catal Sci Technol* 4:142–151. <https://doi.org/10.1039/C3CY00594A>
- Rao CNR, Natarajan S, Vaidhyanathan R (2004) Metal carboxylates with open architectures. *Angew Chem* 43:1466. <https://doi.org/10.1002/anie.200300588>
- Rostamizadeh S, Daneshfar Z, Moghimi H (2019) Synthesis of sulfamethoxazole and sulfabenzamide metal complexes;

- evaluation of their antibacterial activity. *Eur J Med Chem* 171:364. <https://doi.org/10.1016/j.ejmech.2019.03.002>
30. Safajoo N, Mirjalili BBF, Bamoniri A (2019) Fe₃O₄@nano-cellulose/ Cu (II): a bio-based and magnetically recoverable nano-catalyst for the synthesis of 4H-pyrimido [2,1-b] benzothiazole derivatives. *RSC Adv* 9:1278. <https://doi.org/10.1039/C8RA09203F>
 31. Safari J, Banitaba SH, Khalili SD (2011) Cellulose sulfuric acid catalyzed multicomponent reaction for efficient synthesis of 1,4-dihydropyridines via unsymmetrical hantzsch reaction in aqueous media. *J Mol Catal A* 335:46–50. <https://doi.org/10.1016/j.molcata.2010.11.012>
 32. Sarnikar P, Mane YD, Survarse SM, Khade BC (2015) Samarium chloride: an efficient catalyst synthesis of 1, 4-dihydropyridines (Hantzsch pyridines). *Der Pharma Chem* 7:1–4
 33. Shukla SK, Mishra AK, Arotiba OA, Mamba BB (2013) Chitosan-based nanomaterials: a state-of-the-art review. *Int J Biol Macromol* 59:46–58. <https://doi.org/10.1016/j.ijbiomac.2013.04.043>
 34. Soliman AA, Mohamed GG, Hosny WM, Mawgood MAE (2005) Synthesis, spectroscopic and thermal characterization of new sulfasalazine metal complexes. *Synth React Inorg Metal-organic Nano-metal Chem* 35:483–490. <https://doi.org/10.1081/SIM-200067043>
 35. Tamadon F, Moradi S (2013) Controllable selectivity in Biginelli and hantzsch reactions using nano ZnO as a structure base catalyst. *J Mol Catal A* 370:117–122. <https://doi.org/10.1016/j.molcata.2012.12.005>
 36. Valkenber MH, Hölderich WF (2002) Preparation and use of hybrid organic–Inorganic catalysts. *Catal. Reviews* 44:321–374. <https://doi.org/10.1081/CR-120003497>
 37. Witte EC (1986) 7-(Piperazinylpropoxy) - 2H-1-benzo-pyran-2-ones Ger Offen DE 3427985. *Chem Abstr* 104:224915f
 38. Zarnegar Z, Safari J (2014) Fe₃O₄@chitosan nanoparticles: a valuable heterogeneous nano catalyst for the synthesis of 2, 4, 5-trisubstituted imidazoles. *RSC Adv* 4:20932–20939. <https://doi.org/10.1039/C4RA03176H>
 39. Zhang M, Liu P, Liu YH, Shang ZR, Hu HC, Zhang ZH (2016) Magnetically separable graphene oxide anchored sulfonic acid: a novel, highly efficient and recyclable catalyst for one-pot synthesis of 3,6-di(pyridin-3-yl)-1H-pyrazolo[3,4-b]pyridine-5-carbonitriles in deep eutectic solvent under microwave irradiation. *RSC Adv* 6:106160. <https://doi.org/10.1039/C6RA19579B>
 40. Zhang HY, Hao XP, Mo LP, Liu SS, Zhang WB, Zhang ZH (2017) A magnetic metal–organic framework as a highly active heterogeneous catalyst for one-pot synthesis of 2-substituted alkyl and aryl (indolyl) kojic acid derivatives. *New J Chem* 41:7108–7115. <https://doi.org/10.1039/C7NJ01592E>
 41. Zhang M, Fu QY, Gao G, He HY, Ying Zhang WuYS, Zhang ZH (2017) Catalyst-Free, visible-light promoted one-pot synthesis of spirooxindole-pyran derivatives in aqueous ethyl lactate. *ACS Sustain Chem Eng* 5:6175. <https://doi.org/10.1021/acssuschemeng.7b01102>
 42. Zhang M, Liu YH, Shang RZ, Hu HC, Zhang ZH (2017) Supported molybdenum on graphene oxide/Fe₃O₄: an efficient, magnetically separable catalyst for one-pot construction of spiro-oxindole dihydropyridines in deep eutectic solvent under microwave irradiation. *Catal Commun* 88:39. <https://doi.org/10.1016/j.catcom.2016.09.028>
 43. Zhao XN, Hu GF, Tang M, Shi TT, Guo XL, Li TT, Zhang ZH (2014) A highly efficient and recyclable cobalt ferrite chitosan sulfonic acid magnetic nanoparticle for one-pot, four-component synthesis of 2H-indazolo [2,1-b] phthalazine-triones. *RSC Adv* 25:12929–12943. <https://doi.org/10.1039/C4RA09984B>
 44. Zhao XN, Hu HC, Zhang FJ, Zhang ZH (2014) Magnetic CoFe₂O₄ nanoparticle immobilized N-propyl diethylenetriamine sulfamic acid as an efficient and recyclable catalyst for the synthesis of amides via the Ritter reaction. *Appl Catal A* 482:258–265. <https://doi.org/10.1016/j.apcata.2014.06.006>
 45. Zonouz MA, Eskandari I, Moghani D (2012) Acceleration of multicomponent reactions in aqueous medium: multicomponent synthesis of a 4H-pyran library. *Chem Sci Trans* 1(1):91–102. <https://doi.org/10.7598/cst2012.143>

Publisher's Note Springer Nature remains neutral with regard to jurisdictional claims in published maps and institutional affiliations.